

The elongation rate of RNA polymerase II in zebrafish and its significance in the somite segmentation clock

Anja Hanisch^{1,*}, Maxine V. Holder^{1,*}, Suma Choorapoikayil^{2,3}, Martin Gajewski^{2,4}, Ertuğrul M. Özbudak^{5,†} and Julian Lewis^{1,†}

SUMMARY

A gene expression oscillator called the segmentation clock controls somite segmentation in the vertebrate embryo. In zebrafish, the oscillatory transcriptional repressor genes *her1* and *her7* are crucial for genesis of the oscillations, which are thought to arise from negative autoregulation of these genes. The period of oscillation is predicted to depend on delays in the negative-feedback loop, including, most importantly, the transcriptional delay – the time taken to make each molecule of *her1* or *her7* mRNA. *her1* and *her7* operate in parallel. Loss of both gene functions, or mutation of *her1* combined with knockdown of *Hes6*, which we show to be a binding partner of *Her7*, disrupts segmentation drastically. However, mutants in which only *her1* or *her7* is functional show only mild segmentation defects and their oscillations have almost identical periods. This is unexpected because the *her1* and *her7* genes differ greatly in length. We use transgenic zebrafish to measure the RNA polymerase II elongation rate, for the first time, in the intact embryo. This rate is unexpectedly rapid, at 4.8 kb/minute at 28.5°C, implying that, for both genes, the time taken for transcript elongation is insignificant compared with other sources of delay, explaining why the mutants have similar clock periods. Our computational model shows how loss of *her1* or *her7* can allow oscillations to continue with unchanged period but with reduced amplitude and impaired synchrony, as manifested in the *in situ* hybridisation patterns of the single mutants.

KEY WORDS: Somite, Segmentation clock, Zebrafish, *her1*, *her7*, RNA polymerase II

INTRODUCTION

The pace of embryonic development and differentiation depends on the delays involved in switching gene activities on or off. These delays are generally difficult to measure in the intact organism. In some situations, however, genes switch on and off repeatedly in a regular, oscillatory fashion. The period of oscillation – the length of a tick of the molecular clock – is then a precisely defined measurable quantity. Such oscillations are typically driven by delayed negative feedback in the control of gene expression, and the length of the period reflects the length of the delays in the feedback loop. To understand how such a gene expression clock works, we need to know how and where the delays occur. Examination of this question not only leads to an understanding of the oscillator, but also provides insight into the nature and magnitude of gene switching delays in general.

The segmentation clock is a prime example of this type of system. This gene expression oscillator governs demarcation of the boundaries between the embryonic rudiments of the vertebrate body axis, the somites, which are generated sequentially in head-to-tail order from the presomitic mesoderm (PSM) at the tail end of the embryo (Palmeirim et al., 1997; Pourquié, 2011). Each somite consists of the cohort of cells that emerge from the PSM in the course of one oscillation cycle. Thus, the cyclic operation of the

segmentation clock is recorded, writ large, in the spatially periodic structure of the vertebral column.

The set of oscillatory genes varies between species (Krol et al., 2011), but in all species includes member(s) of the *hairy/E(spl)* family as the one common element. In zebrafish, two linked members of this family, *her1* and *her7* (Gajewski et al., 2000), have been identified as central to the genesis of oscillations. When both are deleted (Henry et al., 2002) or blocked by morpholinos (Gajewski et al., 2003; Henry et al., 2002; Oates and Ho, 2002) all signs of oscillation are lost and segment boundary formation is disrupted all along the body axis. Although other members of the *Her* gene family, including *her2*, *her4*, *her12* and *her15* (Krol et al., 2011; Shankaran et al., 2007; Sieger et al., 2004), also display oscillatory expression in the zebrafish PSM, none of these has so far been shown to be essential for operation of the clock in the same way as *her1* and *her7*.

her1 and *her7* encode bHLH inhibitory transcriptional regulators that negatively regulate their own expression and that of each other (Giudicelli et al., 2007; Holley et al., 2002; Oates and Ho, 2002). Mathematical modelling has demonstrated that direct autoinhibition of *her1* and *her7* by their own products could be the mechanism that gives rise to oscillating gene expression (Fig. 1), provided that certain conditions are satisfied (Lewis, 2003). In particular, the transcriptional and translational delays are critical – that is, the time T_m taken to make each molecule of *her1* or *her7* mRNA, from initiation of transcription to delivery into the cytoplasm, and the time T_p from initiation of translation of each molecule of *Her1* or *Her7* protein to its arrival at its binding site in the nucleus. For sustained oscillations, the lifetimes τ_m and τ_p of the mRNA and protein molecules must be short compared with the sum of these delays. If the conditions for oscillation are met, the period of oscillation, T , to a good approximation is given by:

$$T=2(T_m + T_p + \tau_m + \tau_p).$$

¹Vertebrate Development Laboratory, Cancer Research UK London Research Institute, 44 Lincoln's Inn Fields, London WC2A 3LY, UK. ²Institute for Genetics, University of Cologne, Zùlpicher Str. 47a, D-50674 Cologne, Germany. ³Hubrecht Institute, Uppsalalaan 8, 3584 CT Utrecht, The Netherlands. ⁴Hamilton Bonaduz AG, Via Crusch 8, 7402 Bonaduz, Switzerland. ⁵Department of Genetics, Albert Einstein College of Medicine, Bronx, New York, NY 10461, USA.

*These authors contributed equally to this work

†Authors for correspondence (ertugrul.ozbudak@einstein.yu.edu; julian.lewis@cancer.org.uk)

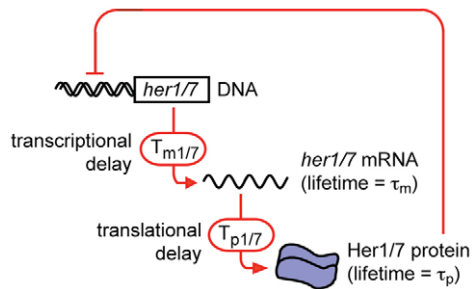


Fig. 1. The proposed core gene circuit of the zebrafish segmentation clock. Oscillations arise from delayed negative-feedback regulation of the *her1* and *her7* genes by their own protein products.

This formula is derived for the idealised case of a single '*her1/7*' autoinhibitory gene or, equivalently, of a pair of genes, *her1* and *her7*, that have the same delays, lifetimes and regulation. Computer modelling shows that if *her1* and *her7* have somewhat different delays and lifetimes but are co-regulated, oscillations will occur with a period that is a compromise between that for a pure *her1* oscillator and that for a pure *her7* oscillator. Mutants in which *her1* remains intact but *her7* is functionally null, or vice versa, have recently become available, and in this paper we use them to test this prediction. Because the *her1* and *her7* genes are very different in length (Fig. 2A), we anticipated that they should have different transcriptional delays, leading to different periods of oscillation. To our surprise, we found that the difference of period is actually very small. To resolve this paradox, we measured the elongation rate of RNA polymerase II (RNA Pol II), for the first time *in vivo* in a vertebrate. The value, as measured in the PSM cells of the zebrafish, is 4.8 kb/minute at 28.5°C. This unexpectedly high rate means that the time taken to transcribe the two genes is so short as to be insignificant in comparison with other sources of delay, such as the time required for splicing. These findings reconcile our theory with the experimental observations and remove an important objection to the proposition that *her1* and *her7* are pacemakers of the segmentation clock.

MATERIALS AND METHODS

Ethics statement

Animal experiments were approved by the CRUK London Research Institute Ethical Review Committee (ref. JLE1706) and the UK Home Office (Project Licence 80/2081 held by J.L.).

Fish stocks, mutant and transgenic fish lines

Adult zebrafish (*Danio rerio*) were kept on a regular light-dark cycle (14 hours on/10 hours off) at 27°C. Embryos were maintained at 28.5°C. The *her1*^{hu2124} and *her7*^{hu2526} mutant lines (Busch-Nentwich et al., 2010) (S. Choorapokayil, PhD Thesis, University of Cologne, 2008; C. Schröter, PhD Thesis, Technische Universität Dresden, 2010) were generated at the Hubrecht Laboratory as part of the ZF-MODELS project. *b567* was a gift from Sharon Amacher (Henry et al., 2002).

The *b21* DNA construct used for the generation of *TgBAC_BX537304(her1:d1EGFP)cj1* transgenic fish was created by standard recombination techniques (Liu et al., 2003) using CH211-283H6 (<http://bacpac.chori.org/>) as the host BAC. This BAC contains the complete *her1/7* locus plus adjacent sequences. The *her7* second intron was split into two halves by insertion of intronic DNA from human dystrophin (*DMD*) intron 74-75 (excluding the first 300 and last 324 bases, total length 21.3 kb). *d1EGFP* (Clontech) was inserted in place of the translated region of *her1*, preserving *her1* 5' and 3' UTRs. The BAC construct included an I-

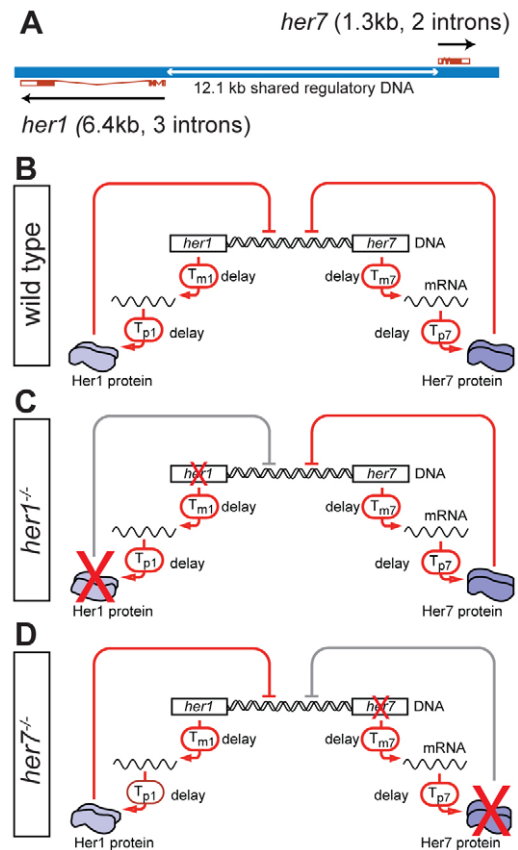


Fig. 2. Differences in *her1* and *her7* gene length might be expected to lead to differences in transcriptional delay. (A) The genomic locus of zebrafish *her1* and *her7*. Black arrows indicate direction of transcription. (B–D) The *her1/7* feedback loops in wild-type (B), *her1*^{−/−} (C) and *her7*^{−/−} (D) embryos.

SceI site to facilitate integration. The transgenic fish were generated by injection of the DNA (with I-*SceI* meganuclease) into fertilised eggs as described previously (Ozbudak and Lewis, 2008). We confirmed by PCR that the entire modified *her7* locus, including the inserted intronic sequence, was present in the transgenic fish (supplementary material Fig. S2). The transgene has now been transmitted in simple Mendelian fashion through many generations and is clearly present only at a single locus in the genome, as is also evident from the number of nuclear dots marking sites of transcription of the transgene in fluorescent *in situ* hybridisation (FISH) specimens.

Probes and *in situ* hybridisation

We used RNA probes for published genes as follows: *her1* (Takke and Campos-Ortega, 1999), *her7* (Henry et al., 2002; Oates and Ho, 2002), *deltaC* (Jiang et al., 2000) and *cb1045* (*xirp2a* – Zebrafish Information Network) (Riedel-Kruse et al., 2007). To detect the different parts of the artificial intron in the *b21* transgenic fish, we used two intronic probes: probe A11 (899 nt) is complementary to the initial part of the artificial *DMD* intron in the *her7*^{b21} transgene, from nt 551 of the intron to nt 1450; probe A12 (998 nt) recognises a middle segment of that intron, from nt 10,953 of the intron to nt 11,951.

For non-fluorescent ISH we used standard NBT/BCIP protocols (Oxtoby and Jowett, 1993). For FISH, specimens were hybridised with fluorescein-labelled probes and, in the case of double FISH, simultaneously with digoxigenin-labelled probes according to standard protocols. Bound fluorescein-labelled probe was detected using peroxidase-conjugated anti-fluorescein sheep antibody (Perkin Elmer; 1/125) and the TSA Plus Fluorescein system (Perkin Elmer). For double FISH, peroxidase activity

was then destroyed by a dehydration series in methanol and incubation for 30 minutes in 100% methanol with 1% H₂O₂, followed by rehydration. Then, embryos were incubated with peroxidase-conjugated anti-digoxigenin mouse antibody (Jackson ImmunoResearch Laboratories; 1/1000) and peroxidase activity was detected using the TSA Plus Cyanine 3 system (Perkin Elmer). Specimens were counterstained with DAPI, mounted in SlowFade Gold (Invitrogen), and imaged with a Zeiss LSM700 or LSM510 confocal microscope.

Immunoprecipitation and western blotting

Full-length cDNAs of *her1*, *her7*, *hes6* and *mib* were cloned in-frame 3' with 6×Myc tag or 1×FLAG tag coding sequences, with an additional linker sequence encoding amino acids GAGAGA interposed between the 5' tag and the start codon. The pCS2+MT vector (<http://sitemaker.umich.edu/dltturner.vectors/home>) was used as backbone. All constructs were checked by sequencing.

HEK293 cells were co-transfected with different combinations of plasmids coding for full-length N-terminally tagged Her1, Her7, Hes6 and Mib using TransIT-LT1 reagent (Mirus Bio). Forty-eight hours after transfection, cells were harvested in lysis buffer (50 mM Hepes pH 7.4, 175 mM NaCl, 0.5% Triton X-100, 0.03 µg/µl DNase and RNase). For immunoprecipitation, cell extracts were incubated with protein G Sepharose beads (Sigma) and anti-Myc 9E10 monoclonal antibody (CRUK LRI Cell Services). For western blots, we used either rabbit anti-FLAG or the anti-Myc 9E10 antibody and the ECL+Plus western blotting detection system (GE Healthcare).

Calcein staining and vertebra counts

Living zebrafish aged 21–28 days were immersed in calcein solution [Sigma-Aldrich, 21030-1G; 0.2% (w/v) in aquarium water] for 10 minutes, rinsed through several containers of clean aquarium water, and then left to swim in clean aquarium water for at least a further 30 minutes, during which time they lost calcein from their soft tissues leaving only their skeletons stained. To count vertebrae, fish were anaesthetised in tricaine solution and observed under fluorescence illumination using a Leica Fluo III stereomicroscope with FITC filter set. We counted the first Weberian vertebra as vertebra 1 and the urostyle as the last vertebra (Bird and Mabee, 2003).

Mathematical modelling

We used Mathematica (Wolfram Research) for computer modelling of *her1/her7* segmentation clock dynamics. We extended our previous two-cell model (Lewis, 2003) to simulate an array of many cells with noisy oscillatory dynamics, with parameters roughly as in Giudicelli et al. (Giudicelli et al., 2007) and with Notch signalling assumed to work as in Ozbudak and Lewis (Ozbudak and Lewis, 2008) to keep neighbouring cells synchronised. Noise arises in the model from the stochastic nature of the association/dissociation reaction between the regulatory proteins and the regulatory DNA, modelled explicitly as a probabilistic (random) process (Lewis, 2003). The model is adjusted to take account of the evidence that Her7 functions as a heterodimer with Hes6; this involves a slightly changed assumption about the stoichiometry of gene regulation by Her1 and Her7, with Her7 binding to the regulatory DNA as a pair of heterodimers with Hes6 (i.e. as a Her₂Hes₂ complex). For details of the model, the Mathematica program and output (including Movies 1 and 2), see supplementary material Model 1.

RESULTS

In *her1*^{-/-} and *her7*^{-/-} mutants, oscillations of gene expression in the PSM are disturbed but somite defects are mild

Morpholino experiments (Gajewski et al., 2003; Henry et al., 2002; Holley et al., 2002; Oates and Ho, 2002) have indicated that loss of function of *her1* or *her7* leads to segmentation defects, affecting anterior somites for *her1* and posterior somites for *her7*, but in each case allowing some regions of normal segmentation. However, morpholinos can have misleading effects. We have therefore re-examined these results using loss-of-function mutants.

The mutant alleles *her1*^{hu2124} and *her7*^{hu2526} have point mutations that create stop codons in the HLH dimerisation domain (for *her1*^{hu2124}, S46>Stop; for *her7*^{hu2526}, K37>Stop). Both are therefore expected to be functionally null. Homozygotes of each type are viable but have reduced fertility. To compare homozygous embryos with wild-type and heterozygous siblings, we examined progeny of homozygote × heterozygote or heterozygote × heterozygote crosses. In each batch of embryos, a subset was clearly abnormal when analysed by ISH, corresponding to the expected Mendelian proportion of homozygotes with 100% penetrance. We took these to be the homozygotes.

A full description of the *her1*^{hu2124} and *her7*^{hu2526} phenotypes is given elsewhere (Choorapoikayil et al., 2012); here we describe the main features relevant to our present theme. The segmentation phenotypes of the homozygotes are compared with those of the wild type in Fig. 3A–C. In *her1* mutant embryos, we saw no segmentation defects apart from occasionally irregular boundaries of the anteriormost somites (Fig. 3B). In *her7* mutant embryos, anterior somite boundaries up to at least the tenth were unaffected; defects were confined to the posterior trunk and tail region, where somite boundaries were still visible and for the most part properly spaced, but often irregular, broken or incomplete (Fig. 3C). Individual embryos of the same mutant genotype varied in the extent of segmentation defects (supplementary material Fig. S1). These abnormalities are similar to those reported in morphants (Gajewski et al., 2003; Henry et al., 2002; Oates and Ho, 2002), although somewhat less severe.

Despite the mildness of the segmentation phenotypes, the expression patterns of segmentation clock components in each of the mutants were distinctly abnormal in much the same way as reported previously for morphants. We assessed these patterns by ISH in whole mounts, using both standard NBT/BCIP staining (Fig. 3D–L'), for comparison with previous studies, and tyramide chemistry with fluorescent detection (Fig. 3M–U'), which allowed optical sectioning. Three main points emerged. First, both *her1*^{-/-} and *her7*^{-/-} mutants show clear signs of continuing coordinated oscillation in the expression of all three oscillatory genes (*her1*, *her7* and *deltaC*) as manifest in variation between siblings (reflecting fixation in different phases of the oscillator cycle) and in the presence of stripes (for *her7* and *deltaC* at least) in the anterior PSM. Second, the number of PSM stripes is reduced, especially in the *her1*^{-/-} mutants (compare Fig. 3G–I' with 3D–F' and 3P–R' with 3M–O'). This implies that the process of oscillator slowing prior to arrest as cells approach the anterior boundary of the PSM is spread out over a smaller number of oscillator cycles [supplementary information Box 2 in Gomez et al. (Gomez et al., 2008)]. In other words, the cells halt their cycling more abruptly than in wild type. Third, in the *her7*^{-/-} mutants the ISH pattern, especially that of *her1* (Fig. 3J,J',S,S'), is less regular and more noisy than normal and shows less variation between siblings, hinting at some loss of cell-cell synchronisation.

Hes6 is required as a binding partner for Her7

Combined loss of function of *her1* and *her7* results in a failure of regular somite boundary formation all along the embryonic body axis and in failure of the oscillations of *deltaC* (Gajewski et al., 2003; Henry et al., 2002; Oates and Ho, 2002). Interestingly, however, double knockdown of *her1* and the non-cyclic gene *hes6* (*her13.2*) results in the same severe segmentation phenotype (Sieger et al., 2006). Her1 and Hes6 proteins have been reported to bind to one another (Kawamura et al., 2005), suggesting that Hes6 might be required for the function of Her1 and/or Her7. To clarify

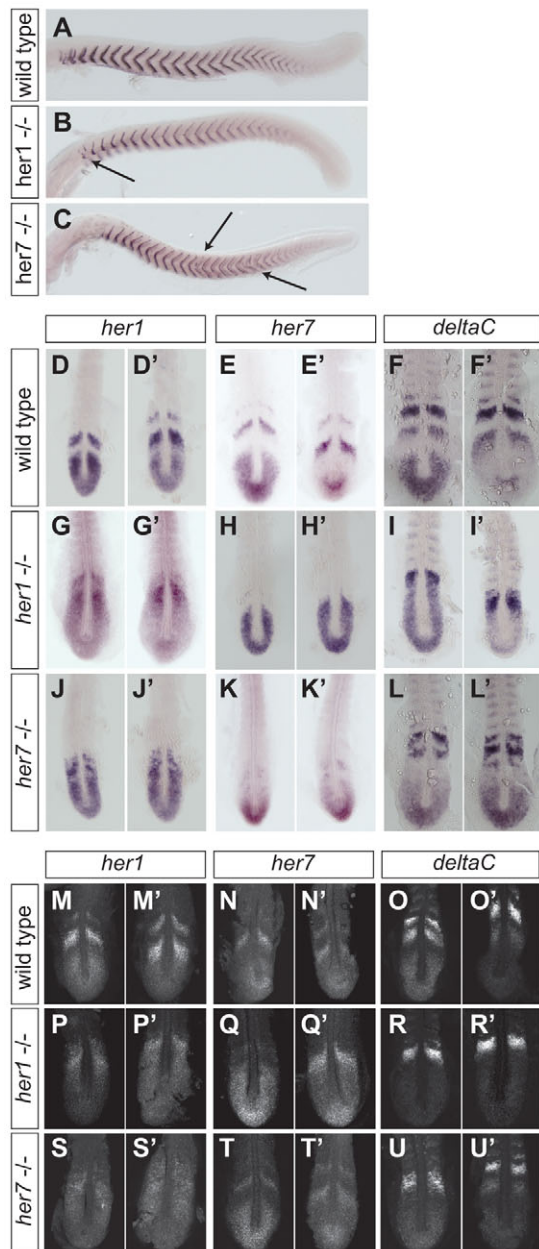


Fig. 3. *her1*^{-/-} and *her7*^{-/-} embryos show mild defects in somite boundary formation and disturbed expression of oscillatory genes in the PSM. (A-C) Zebrafish embryos fixed at ~24 hpf and stained with *cb1045* ISH probe to show somite boundaries (lateral views). (A) Wild type (siblings of *her7*^{-/-} mutant); (B) *her1*^{-/-}; (C) *her7*^{-/-}. Arrows indicate irregularities of segmentation. **(D-U')** Expression patterns of *her1*, *her7* and *deltaC* in wild type, *her1*^{-/-} and *her7*^{-/-} as shown by conventional ISH (D-L') and FISH (M-U'; optical sections). Embryos are at the 10-somite stage (14 hpf) and flat mounted. Two specimens from each cohort are shown to illustrate the oscillatory behaviour. Note that the ISH phenotype, like the segmentation phenotype (supplementary material Fig. S1), varied in severity from one batch of embryos to another (compare K,K' with T,T'). A total of 243 embryos were stained and assessed, including at least 12 for each gene/genotype combination.

this situation, we transiently transfected HEK293T cells with expression constructs coding for tagged versions of Her1, Her7 and Hes6, and analysed their patterns of association by co-

immunoprecipitation. In this overexpression situation, we saw all possible homo- and heterodimeric combinations of Her1, Her7 and Hes6, but with very different preferences: whereas Her1 preferentially homodimerised, Her7 mainly heterodimerised with Hes6 (Fig. 4A).

Thus, in contrast to the previous report (Kawamura et al., 2005), our *in vitro* data suggest that Her1 functions mainly as a homodimer, whereas Her7 functions mainly as a heterodimer with Hes6. Our findings agree with recent data from Trofka et al. (Trofka et al., 2012) (published after the initial submission of our manuscript): they analysed the dimerisation of a larger set of zebrafish Her family proteins, and similarly concluded that the functional dimers are Her1-Her1 homodimers and Her7-Hes6 heterodimers. This explains why deficiency of *her1* and *hes6*, but not deficiency of *her7* and *hes6*, gives the same segmentation phenotype as deficiency of *her1* and *her7* (Sieger et al., 2006) (Fig. 4B). These findings are consistent with the idea that *her1* and *her7* are the central oscillatory components of the segmentation clock but function quasi-redundantly.

***her1* and *her7* are each capable, in the absence of the other, of sustaining oscillations with almost exactly the normal period**

According to our previous theory (Lewis, 2003), the period of oscillation of the segmentation clock should depend on the delay in the *her1/her7* negative-feedback loop, and a major component of the delay is expected to be the time taken to make a mature transcript. However, the *her1* and *her7* genes differ substantially in length (6392 bp and 1304 bp, respectively, from the start of the 5' UTR to the end of the 3' UTR) (Fig. 2A); thus, one might expect that they should have different transcriptional delays. A commonly quoted textbook value (e.g. Alberts et al., 2008) for the RNA Pol II elongation rate is 1.2 kb/minute, implying that transcription of *her1* should take 4.25 minutes longer than that of *her7*. This discrepancy, by itself, would entail that the period of a pure *her1* oscillator should be ~8.5 minutes longer than that of a pure *her7* oscillator, with the period of the full *her1/her7* oscillator lying somewhere in between (Fig. 2B). Assuming that the total duration of somitogenesis is independent of *her1* and *her7*, this line of argument would imply that the total number of somites generated should be substantially larger (~15%, corresponding to four or five additional somites) for a *her1* mutant than for a *her7* mutant.

This is not what we found. We counted the number of segments in *her1*^{-/-} and *her7*^{-/-} mutants, both in 48-hpf embryos stained by ISH for the somite boundary marker *cb1045* (Riedel-Kruse et al., 2007) (Fig. 3A-C; supplementary material Fig. S1) and in young fish stained with calcein (Fig. 5). The mean total numbers of somites or vertebrae formed by the mutants were almost identical to the wild-type values, differing by ≤3% (Table 1).

These observations as to the clock period in *her1*^{-/-} and *her7*^{-/-} mutants, as well as our finding that Her7 heterodimerises preferentially with Hes6, agree with the recent findings of Schröter et al. (Schröter et al., 2012), whose paper appeared after the initial submission of our manuscript.

The *b21* line contains a *her7* transgene with normal exons and regulatory elements but an artificially enlarged intron

To test more directly whether the oscillation period actually depends on the length of the *her1* or *her7* gene, and with the aim of obtaining proof that these genes are pacemakers of the clock, we created a transgenic zebrafish line in which the *her7* gene has been

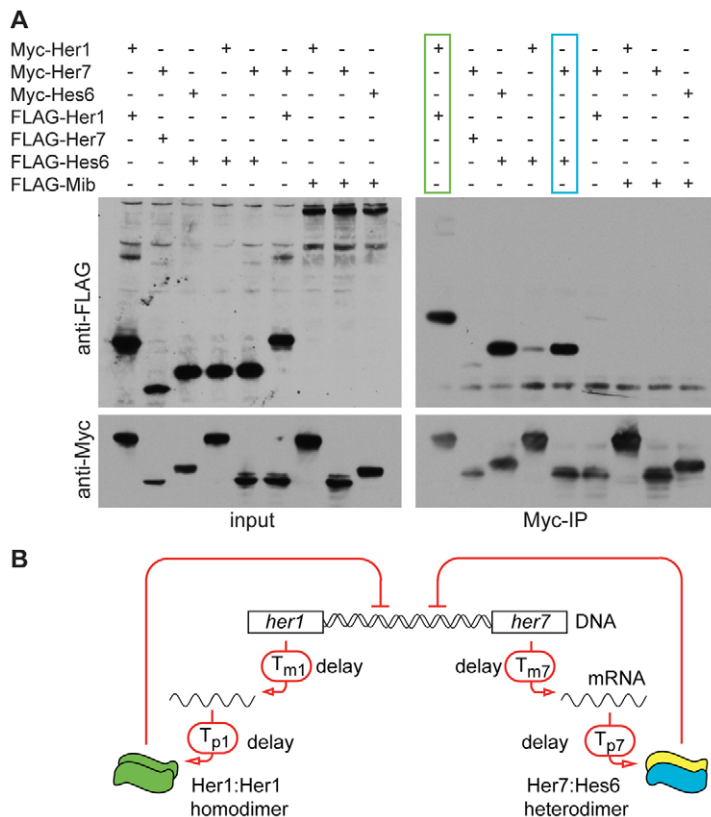


Fig. 4. Her1 preferentially homodimerises, whereas Her7 preferentially heterodimerises with Hes6. (A) HEK293T cells were co-transfected with plasmids encoding either Myc- or FLAG-tagged versions of Her1, Her7, Hes6 and Mib (control), and protein complexes were immunoprecipitated with anti-Myc monoclonal antibody. Cell lysates (input) and immunoprecipitates (Myc-IP) were analysed by western blot using either anti-FLAG (top) or anti-Myc (bottom) antibody. Boxes indicate strongly favoured associations: Her1 homodimerisation (green box) and Her7-Hes6 heterodimerisation (blue box). Note that Hes6 also forms homodimers. **(B)** Negative-feedback loops based on the identified Her protein dimerisation combinations. Her1, green; Her7, blue; Hes6, yellow.

artificially lengthened. For this, we took a BAC containing the full-length *her1* and *her7* genes together with their regulatory DNA, and inserted 21 kb of intronic DNA from the human dystrophin (*DMD*) gene into the second intron of *her7*, creating a modified *her7* gene that we called *her7^{b21}*. To avoid complications from the continued presence of functional *her1*, and to provide, at the same time, a useful fluorescent reporter, we also replaced the *her1* coding sequence with *d1EGFP* (destabilised enhanced GFP; Fig. 6A). We injected the resulting construct into embryos to derive the transgenic line *TgBAC_BX537304(her1:d1EGFP)cj1* or *b21* for short [which we previously used for the *her1:d1EGFP* reporter function (Ozbudak and Lewis, 2008)]. We anticipated that by crossing these with *b567* mutants, which lack endogenous *her1* and *her7* (Henry et al., 2002), we could obtain fish in which oscillations were generated by the *her7^{b21}* transgene acting alone, with a period that was altered according to the extra time required for transcription of the giant intron.

Although we succeeded in creating *b21;b567^{-/-}* embryos, the *her7^{b21}* transgene failed to rescue the *b567* deficiency. The giant intron failed to be spliced out correctly, almost no normal *her7* mRNA was produced, and we were unable to detect any sign of oscillations (data not shown).

Spatial offsets of the *in situ* hybridisation patterns with different probes allow the measurement of relative delays in transcription

The *b21* transgenic line did, however, enable us to measure how fast RNA Pol II moves as it transcribes a gene in the intact zebrafish embryo – that is, to determine the RNA Pol II elongation rate.

The stripy pattern of expression of the oscillatory genes in the PSM is a manifestation of a slowing of the oscillations as cells are

displaced from the tail bud towards the anterior boundary of the PSM (Lewis, 2003; Palmeirim et al., 1997). The distance from peak to peak of the spatial stripe pattern (the spatial wavelength) corresponds to a phase difference of one complete cycle. If two events within a typical oscillating cell are separated in time by a certain fraction of an oscillation cycle, then they will be seen, in a fixed specimen, in cells separated in space by that same fraction of a spatial wavelength. In this way, knowing the relationship between the period of oscillation and the position of the cells in the PSM, we can use measurements on fixed tissue to deduce the time interval between events of the oscillation cycle (Giudicelli et al., 2007).

This, of course, requires a means of making these events visible. For our present purposes we used fluorescent ISH (FISH) with pairwise combinations of four different probes: probe AI1 (899 nt), which recognises an initial part of the artificially enlarged intron in *her7^{b21}*; probe AI2 (988 nt), which recognises a middle segment of that intron, centred on a point 10,452 nt downstream from the centre of the site recognised by probe AI1 (Fig. 6A); and probes H1 and H7, which are complementary to full-length (spliced) mRNA from the endogenous *her1* and *her7* genes, respectively.

Our main focus was on embryos that contained the *b21* construct but were otherwise wild type. As expected, these embryos possessed a normal functional segmentation clock, manifest in normal somitogenesis and normal stripy PSM patterns of endogenous Her gene expression as revealed with probe H1 (Fig. 6B). This probe recognises both mature *her1* mRNA, located in the cytoplasm, and *her1* pre-mRNA, which is concentrated in nuclear dots at the sites of transcription (Giudicelli et al., 2007; Mara et al., 2007). When we stained embryos in a similar way by FISH with probe AI1 or AI2, we saw intense nuclear dots in a stripy pattern in the PSM, reflecting the presence of intron-

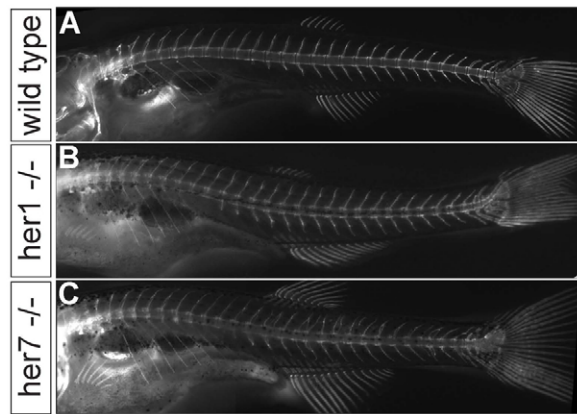


Fig. 5. Wild-type, *her1*^{-/-} and *her7*^{-/-} fish form almost identical numbers of vertebrae. Wild-type (A), *her1*^{-/-} (B) and *her7*^{-/-} (C) fish stained with calcein to visualise calcified tissues. These fish are 21–28 days old and measure 10–12 mm from head to tail. Most *her7*^{-/-} fish have skeletal abnormalities affecting their posterior skeleton, such as missing or bifurcated ribs, irregularly sized vertebrae, and malformation and/or misalignment of the neural and haemal spines. *her1*^{-/-} fish rarely have posterior skeletal defects, but often exhibit defects in their anterior vertebrae (e.g. an extra Weberian vertebra, not visible in this specimen). Mean vertebra counts are the same within 3% for the three genotypes (see Table 1).

containing transcripts at the sites of transcription of the *her7*^{b21} transgene. Double FISH with probes AI1 and H1 (Fig. 6B) or probes AI1 and H7 confirmed that *her7*^{b21} was being transcribed under the control of the segmentation clock, in parallel with the endogenous oscillator genes. Moreover, the anterior boundaries of the stripes of staining with probes AI1 and H1 coincided, implying more or less simultaneous initiation of transcription of the *her7*^{b21} transgene and endogenous *her1*.

In contrast to probes H1 and H7, probe AI1 gave no detectable cytoplasmic staining, implying that the intronic sequence that it recognises was degraded in the nucleus without ever reaching the cytoplasm (Fig. 6B,C). The same appeared to be true of probe AI2, although higher non-specific background made this conclusion less certain. Furthermore, for probe AI1 at least, we saw virtually no diffuse staining in the nuclei: the staining was confined to the dots, strongly suggesting that the pre-mRNA molecules remain associated with the gene from which they are transcribed and do not detach from it until after splicing is complete and the intronic sequence has been degraded. The same phenomenon has been reported by others (Brody et al., 2011; Custódio et al., 1999).

RNA Pol II in zebrafish progresses at 4.8 kb/minute (at 28.5°C)

To estimate the RNA Pol II elongation rate, we took embryos fixed at the 10- to 12-somite stage, stained them by double FISH with probes AI1 and AI2, and compared the distributions of the two sets

of nuclear dots seen in optical sections (Fig. 6C–E). The anterior boundary of each stripe of staining with a given probe reflects the time of onset of production of the pre-mRNA sequence recognised by that probe. The spatial offset between the anterior boundaries of staining with probes AI1 and AI2 therefore reflects the time t_{10kb} taken by RNA Pol II to travel the 10,452 bp from the AI1 site to the AI2 site. We measured this offset from confocal images (Fig. 6) and computed the corresponding time intervals, expressing the result as a fraction of the fundamental clock period T_0 (the time taken to make a somite) (see Materials and methods). In case the labelling and fluorescence detection chemistry might distort the result, we repeated the experiment with the labelling reversed. With probe AI1 detected as red fluorescence and probe AI2 as green, we obtained $t_{10kb}/T_0 = 0.100 \pm 0.008$ (mean \pm s.e.m.; $n=21$). With the labelling reversed, the result was $t_{10kb}/T_0 = 0.088 \pm 0.034$ ($n=8$). Combining these two datasets, we get $t_{10kb}/T_0 = 0.097 \pm 0.011$ ($n=29$). For zebrafish at 28.5°C, $T_0 = 22.6$ minutes (Schröter et al., 2008), implying that the RNA Pol II elongation rate at this temperature is 4.8 ± 0.5 kb/minute.

DISCUSSION

Mathematical modelling predicts oscillations of reduced amplitude and impaired synchrony when *her1* or *her7* is mutated

Our study of the *her1* and *her7* mutants confirms that the two genes function quasi-redundantly in the segmentation clock: whereas loss of both genes disrupts segmentation drastically, when either is functionally null then segments form with only minor irregularities. This was unsurprising and consistent with prevailing theory. We were, however, surprised to see that in the single mutants the expression patterns of *her1*, *her7* and *deltaC* were distinctly abnormal, although they still showed signs of coordinated oscillation. Similar findings have been reported in morphants (Gajewski et al., 2003; Henry et al., 2002; Oates and Ho, 2002). Does the theory explain this aspect of the mutant phenotypes?

To answer this question, we extended our original model (Lewis, 2003; Ozbudak and Lewis, 2008) to describe an array of many oscillatory cells that are individually noisy and coupled and synchronised through Notch signalling (see Materials and methods and supplementary material Model 1). Fig. 7 shows the predictions, comparing the wild type with a mutant in which either *her1* or *her7* is defective. With the chosen parameters, we see that loss-of-function mutation of *her1* or *her7* indeed still permits collective oscillations, but these have impaired synchronisation and reduced peak-to-trough ratio, matching our experimental observations (see Fig. 3).

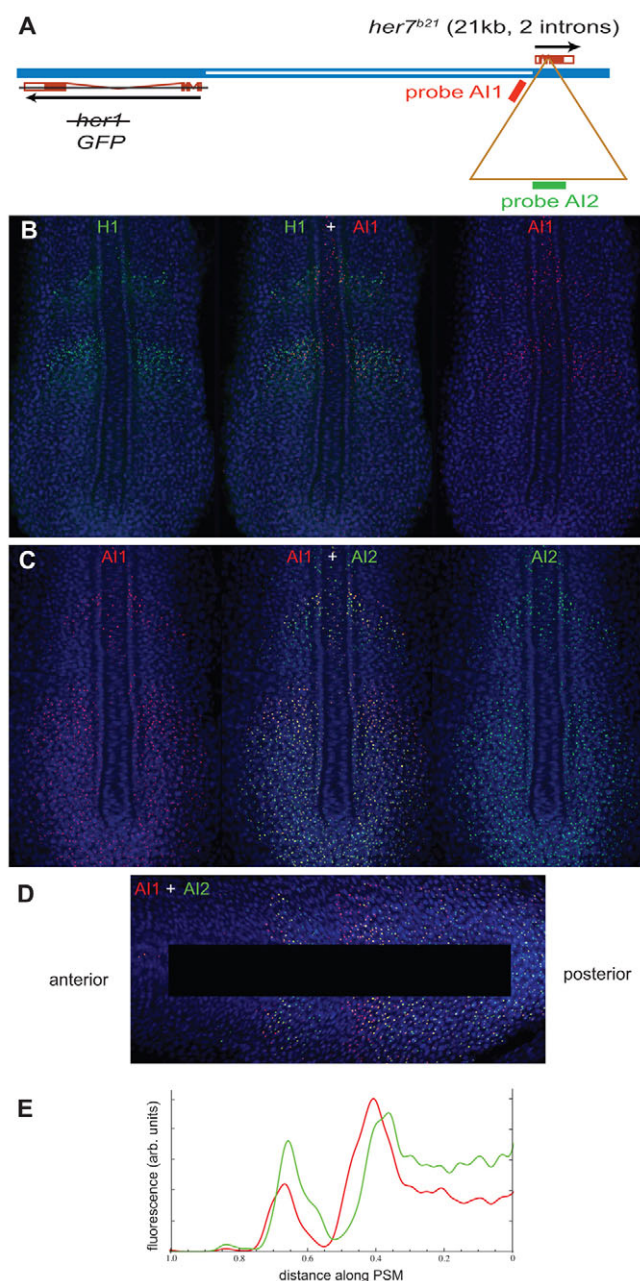
her1 and *her7* remain strong candidates to be joint pacemakers of the segmentation clock

Since *her1* and *her7* differ in length, we expected that they would have different transcriptional delays and that the segmentation clocks of embryos lacking *her1* or *her7* would run, respectively, more quickly or more slowly than those of wild-type embryos,

Table 1. Numbers of vertebrae/segment boundaries in wild-type, *her1*^{-/-} and *her7*^{-/-} zebrafish

	Wild type	<i>her1</i> ^{-/-}	<i>her7</i> ^{-/-}
Calcein-stained juveniles	31.4 \pm 0.5 ($n=228$)	31.5 \pm 0.7 ($n=76$)	32.2 \pm 1.2 ($n=84$)
<i>cb1045</i> ISH of embryos	31.5 \pm 0.8 ($n=226$)	31.0 \pm 1.1 ($n=38$)	30.4 \pm 1.2 ($n=86$)

Shown are the number of segments (mean \pm s.d.) in the three genotypes. Specimens were stained either with calcein as juveniles or by ISH with a *cb1045* probe as 48-hpf embryos. Mutants and wild-type sibling controls were individually genotyped by PCR. The slight ($\leq 3\%$) differences between mutant and wild-type values might reflect inaccuracies in counting segments when these are malformed (see Figs 3, 5); note the increased s.d. for the *her7*^{-/-} mutants.



resulting in the formation of more or fewer segments. But our expectations were confounded: somite and vertebra counts showed there was little difference in the number of segments formed by embryos of the three genotypes, providing a strong indication that their clocks run at practically the same speed. So which part of our theory was wrong?

One questionable assumption was that a major contribution to transcriptional delay came from the time taken by RNA Pol II to transcribe *her1* or *her7* from beginning to end. We measured the RNA Pol II elongation rate in the PSM of intact zebrafish embryos and found that it is much faster than previously supposed. As discussed in detail below, it follows that the time taken for transcript elongation (for *her1* and *her7*) is so short as to make no significant contribution to the total transcriptional delay. This resolves the clash between theory and observation, and means that *her1* and *her7* remain strong candidates to be joint pacemakers of the segmentation clock.

Fig. 6. Measurement of the transcription elongation rate in the PSM of an intact embryo using *b21* transgenic fish. (A) The modified transgenic *her1/7* locus in *b21* fish (compare with Fig. 2A). A ~21 kb artificial intron (brown triangle) was inserted in the second intron of *her7*. Probes AI1 (red) and AI2 (green) recognise regions of this intron that are ~10 kb apart. The *her1* coding sequence is replaced by *d1EGFP*. (B,C) *b21* transgenic embryos fixed at the 10-somite stage (14 hpf) and stained by two-colour FISH with two different probes and with DAPI as nuclear counterstain. Confocal optical sections of the PSM of flat-mounted embryos are shown. The middle image is a merge, with red and green channels shown separately on either side. (B) Co-staining with probes H1 (green; detecting transcripts from endogenous *her1*) and AI1 (red). (C) Co-staining with probes AI1 (red) and AI2 (green). (D) Processed image of the PSM of an embryo co-stained with AI1 and AI2 as used for intensity plot analysis. The image is warped in Adobe Photoshop to make the stripes of gene expression appear at right angles to the body axis, and the notochord and adaxial cells are blanked out leaving only PSM tissue to contribute to the analysis. (E) Intensity of the red and green fluorescence signals as a function of distance along the body axis. For each point along the axis, we took the total signal summed over the transverse column of pixels, and used Gaussian smoothing to obtain a smooth graph. The offset between the red and green signals was measured as the distance between the points of inflection on the rising parts of the curves, and the corresponding timing difference was calculated as described (Giudicelli et al., 2007).

Support for the role of *her1* and *her7* as pacemakers comes from the recent demonstration that the clock period is altered in mutants lacking functional Hes6 (Schröter and Oates, 2010), which we have shown here, in agreement with others (Trofka et al., 2012; Schröter et al., 2012), to be a dimerisation partner of Her7.

It remains conceivable, however, that in conjunction with the *her1/7* transcriptional oscillator and somehow coupled to it, the zebrafish PSM cells might contain an additional molecular oscillator of some different type. The Wnt and Fgf pathway oscillations that occur in parallel with *Hes7* oscillations in the mouse PSM seem to provide an example of this phenomenon (Aulehla et al., 2003; Giudicelli and Lewis, 2004; Dequéant et al., 2006). Studies of circadian clocks have revealed other precedents. For example, the cyanobacterium *Synechococcus* possesses both a transcriptional oscillator and an enzymatic phosphorylation/dephosphorylation oscillator that is independent of transcription; these are normally coupled, but each can generate a circadian rhythm in the absence of the other (Kitayama et al., 2008; Zwicker et al., 2010). Moreover, many organisms, from bacteria to mammals, contain a non-transcriptional oxidation/reduction circadian oscillator that operates in parallel with a transcriptional circadian oscillator (Edgar et al., 2012). Biological clocks, it seems, can have several pacemakers that are loosely coordinated and function together to provide a more reliable measure of time. Thus, while the evidence is compelling that the *her1/7* transcriptional feedback loop is a pacemaker of the zebrafish segmentation clock, it might not be the only one.

The RNA Pol II elongation rate is much faster than previously supposed

We have been able to measure the RNA Pol II elongation rate in the zebrafish embryo by taking advantage of the synchronised waves of transcription that occur during somitogenesis. This is, to our knowledge, the first measurement of this quantity in an intact vertebrate. Our value of 4.8 ± 0.5 kb/minute for zebrafish at 28.5°C is roughly four times faster than estimates commonly quoted in textbooks and reviews (Alberts et al., 2008; Bentley, 2005;

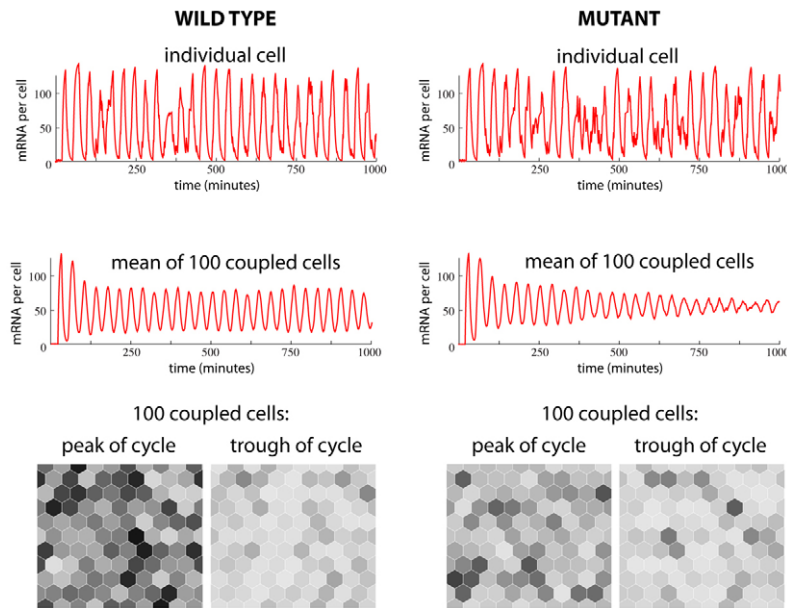


Fig. 7. Mathematical modelling predicts oscillations with reduced amplitude and impaired synchronisation when gene dosage is reduced.

Behaviour of an array of 10×10 noisy *her1/7* cell oscillators coupled by Delta-Notch signalling, modelled as described in the text. Individual cells in the wild type show well-defined but noisy oscillations, and the average over all cells in the array (the collective behaviour) also shows well-defined oscillations because the cells are synchronised. In the *her7* or *her1* mutant, individual cells still oscillate, somewhat more noisily, but the collective oscillation is not only more noisy but also of lower amplitude than in wild type, chiefly because synchronisation is impaired (although not lost). The period is practically unchanged compared with wild type. The bottom panels show the multicellular patterns of gene expression at cycle 14.

Neugebauer, 2002) for eukaryotes in general. It does, however, agree with recent findings for mammalian cells *in vitro*: 4.3 kb/minute (Darzacq et al., 2007); 3.1 kb/minute (Wada et al., 2009); 3.8 kb/minute (Singh and Padgett, 2009); and 3.3 kb/minute (Ben-Ari et al., 2010).

The time taken for transcription is insignificant compared with splicing and export delays

Several steps contribute to the total transcriptional delay T_m : (1) promoter activation; (2) transcription; (3) splicing; (4) 3'-end processing and polyadenylation; (5) release of the transcript from the site of transcription; and (6) exit through a nuclear pore. T_m is not simply the sum of these individual delays, however, because they are not simply sequential. In particular, splicing and transcription occur concurrently, and there is no necessity for splicing of a given intron to be completed before splicing of the next intron downstream can begin (Brody et al., 2011; Kessler et al., 1993; Neugebauer, 2002; Singh and Padgett, 2009; Tennyson et al., 1995; Wada et al., 2009).

At the rate that we have measured, the polymerase should complete the synthesis of pre-mRNA for *her1* (6392 nt) in only 1.6 minutes, for *her7* (1304 nt) in just 0.3 minutes, and for *deltaC* (4854 nt) in only 1.2 minutes. Splicing is likely to be slower. For cultured mammalian cells, reports of the time taken to splice out an intron once it has been transcribed range from 0.4 to 12 minutes, depending on the intron but regardless of intron length (Audibert et al., 2002; Kessler et al., 1993; Singh and Padgett, 2009; Zeisel et al., 2011). A reasonable compromise estimate for the time taken to splice would thus be 5 minutes.

Completion of splicing is coupled with, and may coincide with, completion of 3'-end processing and polyadenylation and release of the transcript from attachment to the gene (steps 4 and 5 above) (Bird et al., 2005; Brody et al., 2011; Custódio et al., 1999). Following this, the time T_{export} (step 6) has been estimated (for β -globin mRNA in 3T3 cells) at 4 minutes (Audibert et al., 2002).

Hence, assuming a splicing delay of 5 minutes and export time of 4 minutes, we arrive at the following theoretical estimates for the total transcriptional delays that occur subsequent to promoter activation:

$$\begin{aligned} T_{\text{mher1}} &= 1.3 \text{ minutes} + T_{\text{sher1}} + T_{\text{export}} \approx 10 \text{ minutes,} \\ T_{\text{mher7}} &= 0.1 \text{ minutes} + T_{\text{sher7}} + T_{\text{export}} \approx 9 \text{ minutes,} \\ \text{and } T_{\text{mdeltaC}} &= 1.0 \text{ minutes} + T_{\text{sdeltaC}} + T_{\text{export}} \approx 10 \text{ minutes,} \end{aligned}$$

where T_{sher1} , T_{sher7} and T_{sdeltaC} are the times taken to splice out the introns from each gene. The first term in each case represents the time taken for the polymerase to complete transcription up to the end of the final intron, at which point splicing of this intron can begin. The splicing reaction (if it takes 5 minutes) will not be completed until after the polymerase has finished transcribing, as the terminal exons of all three genes are relatively short. We assume that introns are spliced concurrently and that the splicing of no single intron is so slow compared with that of the last intron as to be rate limiting.

Given the uncertainties in the extrapolation of splicing times and nuclear export times from cultured mammalian cells to intact zebrafish, these timings should be regarded as rough estimates only. As such, they are consistent with the observed value of the clock period and with our formula for the period as a function of the delays in the negative-feedback loop (Giudicelli et al., 2007; Lewis, 2003). We conclude that there is no reason to expect the period of a pure *her1* oscillator and that of a pure *her7* oscillator to be significantly different.

The splicing delay may be a major determinant of oscillator period and thus of somite spacing and number

Our measurements suggest that the time required to splice out introns constitutes a large component of the total transcriptional delay. Supporting evidence comes from recent experiments (Takashima et al., 2011) focusing on *Hes7*, which is the mouse counterpart of zebrafish *her1* and *her7*. The introns in *Hes7* were found to be responsible for a 19-minute delay in expression of the gene, relative to the expression of an artificial intronless version, and the presence of these introns was shown to be essential for oscillating *Hes7* expression, as expected from the theory if a large part of the transcriptional delay depends on them (Hirata et al., 2004; Lewis, 2003).

The zebrafish segmentation clock shows exceptionally rapid switching of gene expression. We have shown that, even on this

time scale, RNA Pol II moves so rapidly that the time taken to transcribe the oscillator genes is insignificant compared with the other delays and molecular lifetimes that set the tempo of gene switching. The same is likely to be true, even more emphatically, for the generality of gene switching events. Most types of mRNA and protein molecules have a half-life of many hours [median value 9 hours for mammalian mRNAs, 46 hours for mammalian proteins (Schwanhäusser et al., 2011)], whereas the time taken to transcribe a gene of average length [28 kb (Lander et al., 2001; Venter et al., 2001)] should be less than 10 minutes. Thus, gene length is likely to make a negligible contribution to switching delays for the majority of genes, and its contribution is insignificant even in determining the period of the zebrafish segmentation clock.

Acknowledgements

We thank Sharon Amacher for *b567* fish; Michael Stauber for *DMD* intronic DNA; David Ish-Horowicz and Ned Hoyle for discussions; our aquarium staff for excellent fish care; Emel Esen for initial optimisation of FISH for the intronic probes; and Stephan Knierer for help in characterisation of the *b21* transgene insertion.

Funding

The work was funded by Cancer Research UK and EMBO Long-Term Fellowships for A.H. and E.M.Ö.

Competing interests statement

The authors declare no competing financial interests.

Supplementary material

Supplementary material available online at
<http://dev.biologists.org/lookup/suppl/doi:10.1242/dev.077230/-/DC1>

References

- Alberts, B., Johnson, A., Lewis, J., Raff, M., Roberts, K. and Walter, P. (2008). *Molecular Biology of the Cell*. New York, NY: Garland Science.
- Audibert, A., Weil, D. and Dautry, F. (2002). In vivo kinetics of mRNA splicing and transport in mammalian cells. *Mol. Cell Biol.* **22**, 6706-6718.
- Aulehla, A., Wehrle, C., Brand-Saberi, B., Kemler, R., Gossler, A., Kanzler, B. and Herrmann, B. G. (2003). Wnt3a plays a major role in the segmentation clock controlling somitogenesis. *Dev. Cell* **4**, 395-406.
- Ben-Ari, Y., Brody, Y., Kinor, N., Mor, A., Tsukamoto, T., Spector, D. L., Singer, R. H. and Shav-Tal, Y. (2010). The life of an mRNA in space and time. *J. Cell Sci.* **123**, 1761-1774.
- Bentley, D. L. (2005). Rules of engagement: co-transcriptional recruitment of pre-mRNA processing factors. *Curr. Opin. Cell Biol.* **17**, 251-256.
- Bird, N. C. and Mabee, P. M. (2003). Developmental morphology of the axial skeleton of the zebrafish, *Danio rerio* (Ostariophysi: Cyprinidae). *Dev. Dyn.* **228**, 337-357.
- Bird, G., Fong, N., Gatlin, J. C., Farabaugh, S. and Bentley, D. L. (2005). Ribozyme cleavage reveals connections between mRNA release from the site of transcription and pre-mRNA processing. *Mol. Cell* **20**, 747-758.
- Brody, Y., Neufeld, N., Bieberstein, X., Causse, S. Z., Böhnlein, E. M., Neugebauer, K. M., Darzacq, X. and Shav-Tal, Y. (2011). The in vivo kinetics of RNA polymerase II elongation during co-transcriptional splicing. *PLoS Biol.* **9**, e1000573.
- Busch-Nentwich, E., Kettleborough, R., Fenyes, F., Herd, C., Collins, J., de Bruijn, E., van Eeden, F., Cuppen, E. and Stemple, D. L. (2010). Sanger Institute Zebrafish Mutation Resource targeted knockout mutants phenotype and image data submission, Sanger Institute Zebrafish Mutation Resource and Hubrecht Laboratory. *ZFIN Direct Data Submission* (<http://zfin.org>).
- Choorapoikayil, S., Willems, B., Strohle, P. and Gajewski, M. (2012). Analysis of *her1* and *her7* mutants reveals a spatio-temporal separation of the somite clock module. *PLoS ONE* **7**, e39073.
- Custódio, N., Carmo-Fonseca, M., Geraghty, F., Pereira, H. S., Grosveld, F. and Antoniou, M. (1999). Inefficient processing impairs release of RNA from the site of transcription. *EMBO J.* **18**, 2855-2866.
- Darzacq, X., Shav-Tal, Y., de Turris, V., Brody, Y., Shenoy, S. M., Phair, R. D. and Singer, R. H. (2007). In vivo dynamics of RNA polymerase II transcription. *Nat. Struct. Mol. Biol.* **14**, 796-806.
- Dequéant, M. L., Glynn, E., Gaudenz, K., Wahl, M., Chen, J., Mushegian, A. and Pourquié, O. (2006). A complex oscillating network of signaling genes underlies the mouse segmentation clock. *Science* **314**, 1595-1598.
- Edgar, R. S., Green, E. W., Zhao, Y., van Ooijen, G., Olmedo, M., Qin, X., Xu, Y., Pan, M., Valekunja, U. K., Feeney, K. A. et al. (2012). Peroxiredoxins are conserved markers of circadian rhythms. *Nature* **485**, 459-464.
- Gajewski, M., Wolff, C., Rohr, K. B., Wigand, B. and Tautz, D. (2000). *D. rerio her-1* and *her-7* genes. GenBank entry AF292032.
- Gajewski, M., Sieger, D., Alt, B., Leve, C., Hans, S., Wolff, C., Rohr, K. B. and Tautz, D. (2003). Anterior and posterior waves of cyclic *her1* gene expression are differentially regulated in the presomitic mesoderm of zebrafish. *Development* **130**, 4269-4278.
- Giudicelli, F. and Lewis, J. (2004). The vertebrate segmentation clock. *Curr. Opin. Genet. Dev.* **14**, 407-414.
- Giudicelli, F., Ozbudak, E. M., Wright, G. J. and Lewis, J. (2007). Setting the tempo in development: an investigation of the zebrafish somite clock mechanism. *PLoS Biol.* **5**, e150.
- Gomez, C., Ozbudak, E. M., Wunderlich, J., Baumann, D., Lewis, J. and Pourquié, O. (2008). Control of segment number in vertebrate embryos. *Nature* **454**, 335-339.
- Henry, C. A., Urban, M. K., Dill, K. K., Merlie, J. P., Page, M. F., Kimmel, C. B. and Amacher, S. L. (2002). Two linked hairy/Enhancer of split-related zebrafish genes, *her1* and *her7*, function together to refine alternating somite boundaries. *Development* **129**, 3693-3704.
- Hirata, H., Bessho, Y., Kokubu, H., Masamizu, Y., Yamada, S., Lewis, J. and Kageyama, R. (2004). Instability of *Hes7* protein is crucial for the somite segmentation clock. *Nat. Genet.* **36**, 750-754.
- Holley, S. A., Jülich, D., Rauch, G. J., Geisler, R. and Nüsslein-Volhard, C. (2002). *her1* and the notch pathway function within the oscillator mechanism that regulates zebrafish somitogenesis. *Development* **129**, 1175-1183.
- Jiang, Y. J., Aerne, B. L., Smithers, L., Haddon, C., Ish-Horowicz, D. and Lewis, J. (2000). Notch signalling and the synchronization of the somite segmentation clock. *Nature* **408**, 475-479.
- Kawamura, A., Koshida, S., Hijikata, H., Sakaguchi, T., Kondoh, H. and Takada, S. (2005). Zebrafish hairy/enhancer of split protein links FGF signaling to cyclic gene expression in the periodic segmentation of somites. *Genes Dev.* **19**, 1156-1161.
- Kessler, O., Jiang, Y. and Chasin, L. A. (1993). Order of intron removal during splicing of endogenous adenine phosphoribosyltransferase and dihydrofolate reductase pre-mRNA. *Mol. Cell Biol.* **13**, 6211-6222.
- Kitayama, Y., Nishiwaki, T., Terauchi, K. and Kondo, T. (2008). Dual KaiC-based oscillations constitute the circadian system of cyanobacteria. *Genes Dev.* **22**, 1513-1521.
- Krol, A. J., Roellig, D., Dequéant, M. L., Tassy, O., Glynn, E., Hattem, G., Mushegian, A., Oates, A. C. and Pourquié, O. (2011). Evolutionary plasticity of segmentation clock networks. *Development* **138**, 2783-2792.
- Lander, E. S., Linton, L. M., Birren, B., Nusbaum, C., Zody, M. C., Baldwin, J., Devon, K., Dewar, K., Doyle, M., FitzHugh, W. et al. (2001). Initial sequencing and analysis of the human genome. *Nature* **409**, 860-921.
- Lewis, J. (2003). Autoinhibition with transcriptional delay: a simple mechanism for the zebrafish somitogenesis oscillator. *Curr. Biol.* **13**, 1398-1408.
- Liu, P., Jenkins, N. A. and Copeland, N. G. (2003). A highly efficient recombineering-based method for generating conditional knockout mutations. *Genome Res.* **13**, 476-484.
- Mara, A., Schroeder, J., Chalouni, C. and Holley, S. A. (2007). Priming, initiation and synchronization of the segmentation clock by *deltaD* and *deltaC*. *Nat. Cell Biol.* **9**, 523-530.
- Neugebauer, K. M. (2002). On the importance of being co-transcriptional. *J. Cell Sci.* **115**, 3865-3871.
- Oates, A. C. and Ho, R. K. (2002). Hairy/E(spl)-related (Her) genes are central components of the segmentation oscillator and display redundancy with the Delta/Notch signaling pathway in the formation of anterior segmental boundaries in the zebrafish. *Development* **129**, 2929-2946.
- Oxtoby, E. and Jowett, T. (1993). Cloning of the zebrafish *krox-20* gene (*kx-20*) and its expression during hindbrain development. *Nucleic Acids Res.* **21**, 1087-1095.
- Özbudak, E. M. and Lewis, J. (2008). Notch signalling synchronizes the zebrafish segmentation clock but is not needed to create somite boundaries. *PLoS Genet.* **4**, e15.
- Palmeirim, I., Henrique, D., Ish-Horowicz, D. and Pourquié, O. (1997). Avian hairy gene expression identifies a molecular clock linked to vertebrate segmentation and somitogenesis. *Cell* **91**, 639-648.
- Pourquié, O. (2011). Vertebrate segmentation: from cyclic gene networks to scoliosis. *Cell* **145**, 650-663.
- Riedel-Kruse, I. H., Müller, C. and Oates, A. C. (2007). Synchrony dynamics during initiation, failure, and rescue of the segmentation clock. *Science* **317**, 1911-1915.
- Schröter, C. and Oates, A. C. (2010). Segment number and axial identity in a segmentation clock period mutant. *Curr. Biol.* **20**, 1254-1258.
- Schröter, C., Herrgen, L., Cardona, A., Brouhard, G. J., Feldman, B. and Oates, A. C. (2008). Dynamics of zebrafish somitogenesis. *Dev. Dyn.* **237**, 545-553.
- Schröter, C., Ares, S., Morelli, L. G., Isakova, A., Hens, K., Soroldoni, D., Gajewski, M., Julicher, F., Maerkl, S. J., Deplancke, B. et al. (2012). Topology and dynamics of the zebrafish segmentation clock core circuit. *PLoS Biol.* **10**, e1001364.

- Schwanhäusser, B., Busse, D., Li, N., Dittmar, G., Schuchhardt, J., Wolf, J., Chen, W. and Selbach, M. (2011). Global quantification of mammalian gene expression control. *Nature* **473**, 337-342.
- Shankaran, S. S., Sieger, D., Schröter, C., Czepe, C., Pauly, M. C., Laplante, M. A., Becker, T. S., Oates, A. C. and Gajewski, M. (2007). Completing the set of *h/E(spl)* cyclic genes in zebrafish: *her12* and *her15* reveal novel modes of expression and contribute to the segmentation clock. *Dev. Biol.* **304**, 615-632.
- Sieger, D., Tautz, D. and Gajewski, M. (2004). *her11* is involved in the somitogenesis clock in zebrafish. *Dev. Genes Evol.* **214**, 393-406.
- Sieger, D., Ackermann, B., Winkler, C., Tautz, D. and Gajewski, M. (2006). *her1* and *her13.2* are jointly required for somitic border specification along the entire axis of the fish embryo. *Dev. Biol.* **293**, 242-251.
- Singh, J. and Padgett, R. A. (2009). Rates of in situ transcription and splicing in large human genes. *Nat. Struct. Mol. Biol.* **16**, 1128-1133.
- Takashima, Y., Ohtsuka, T., González, A., Miyachi, H. and Kageyama, R. (2011). Intronic delay is essential for oscillatory expression in the segmentation clock. *Proc. Natl. Acad. Sci. USA* **108**, 3300-3305.
- Takke, C. and Campos-Ortega, J. A. (1999). *her1*, a zebrafish pair-rule like gene, acts downstream of notch signalling to control somite development. *Development* **126**, 3005-3014.
- Tennyson, C. N., Klamut, H. J. and Worton, R. G. (1995). The human dystrophin gene requires 16 hours to be transcribed and is cotranscriptionally spliced. *Nat. Genet.* **9**, 184-190.
- Trofka, A., Schwendinger-Schreck, J., Brend, T., Pontius, W., Emonet, T. and Holley, S. A. (2012). The *Her7* node modulates the network topology of the zebrafish segmentation clock via sequestration of the *Hes6* hub. *Development* **139**, 940-947.
- Venter, J. C., Adams, M. D., Myers, E. W., Li, P. W., Mural, R. J., Sutton, G. G., Smith, H. O., Yandell, M., Evans, C. A., Holt, R. A. et al. (2001). The sequence of the human genome. *Science* **291**, 1304-1351.
- Wada, Y., Ohta, Y., Xu, M., Tsutsumi, S., Minami, T., Inoue, K., Komura, D., Kitakami, J., Oshida, N., Papantonis, A. et al. (2009). A wave of nascent transcription on activated human genes. *Proc. Natl. Acad. Sci. USA* **106**, 18357-18361.
- Zeisel, A., Köstler, W. J., Molotski, N., Tsai, J. M., Krauthgamer, R., Jacob-Hirsch, J., Rechavi, G., Soen, Y., Jung, S., Yarden, Y. et al. (2011). Coupled pre-mRNA and mRNA dynamics unveil operational strategies underlying transcriptional responses to stimuli. *Mol. Syst. Biol.* **7**, 529.
- Zwicker, D., Lubensky, D. K. and ten Wolde, P. R. (2010). Robust circadian clocks from coupled protein-modification and transcription-translation cycles. *Proc. Natl. Acad. Sci. USA* **107**, 22540-22545.

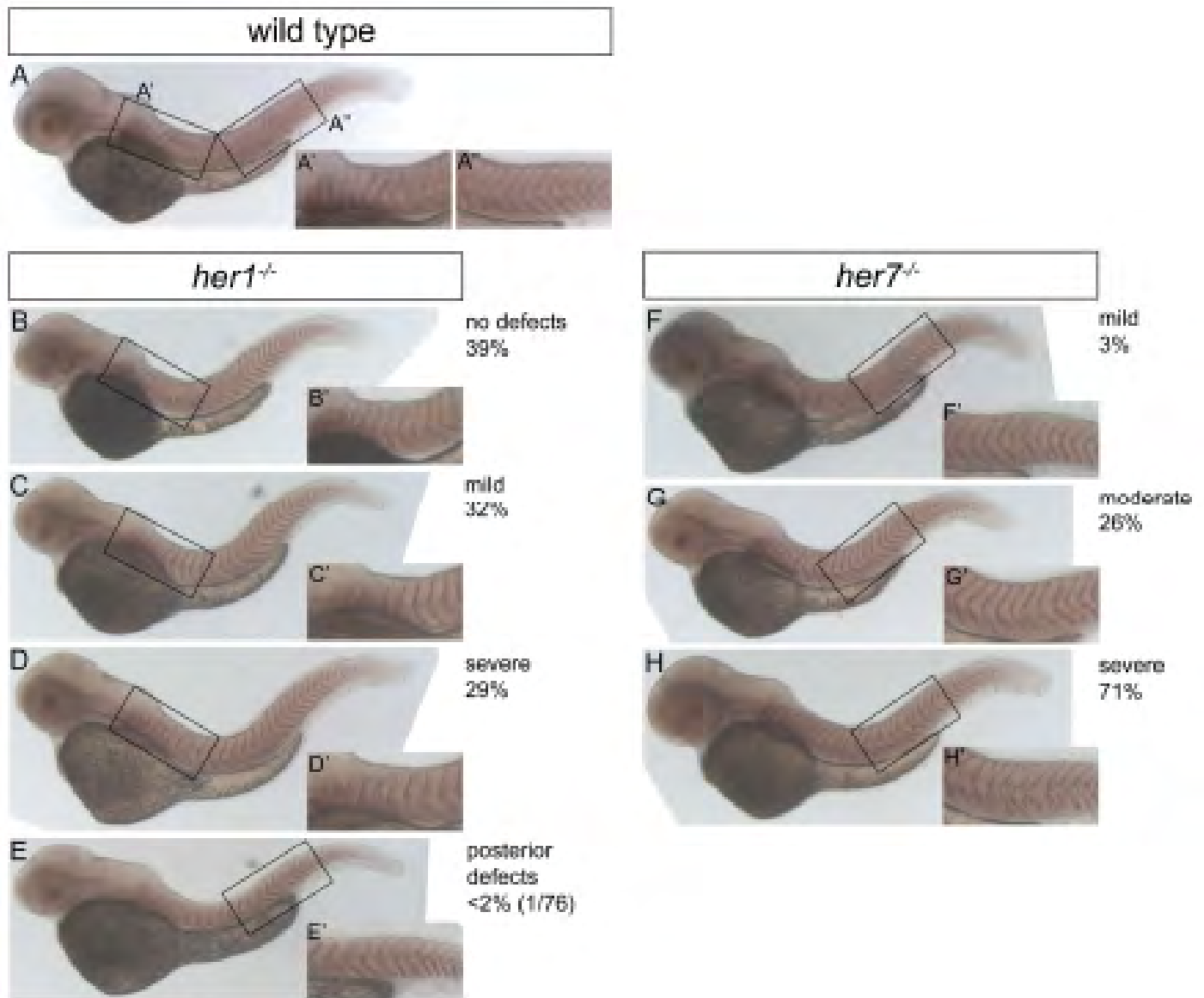


Fig. S1. Variability in the phenotype of *her1*^{-/-} and *her7*^{-/-} embryos. Embryos fixed at 48 hpf and stained with *cb1045* ISH probe to show somite boundaries (lateral views). (A-A'') Wild type; (B-E') *her1*^{-/-} mutant; (F-H') *her7*^{-/-} mutant. Insets show regions affected by segmentation irregularities in more detail. (B-E) A large proportion (~40%) of *her1*^{-/-} embryos show no segmentation defects with the *cb1045* probe. The remaining ~60% of the embryos present one ('mild') or two to three ('severe') absent, broken or abnormally shaped somite boundaries in the anterior of the body. We only found one specimen in which posterior segments were affected (E; *n*=76). (F-H) All *her7*^{-/-} embryos present somite boundary defects (*n*=88). These comprise broken or absent boundaries and boundaries that are misaligned on the two sides of the body. Defects always affect segments in the mid to posterior trunk rather than anterior segments. A small proportion of embryos are almost phenotypically normal ('mild', zero or one segment boundary affected), but most have defects in two to four ('moderate') or more than five ('severe') segment boundaries.

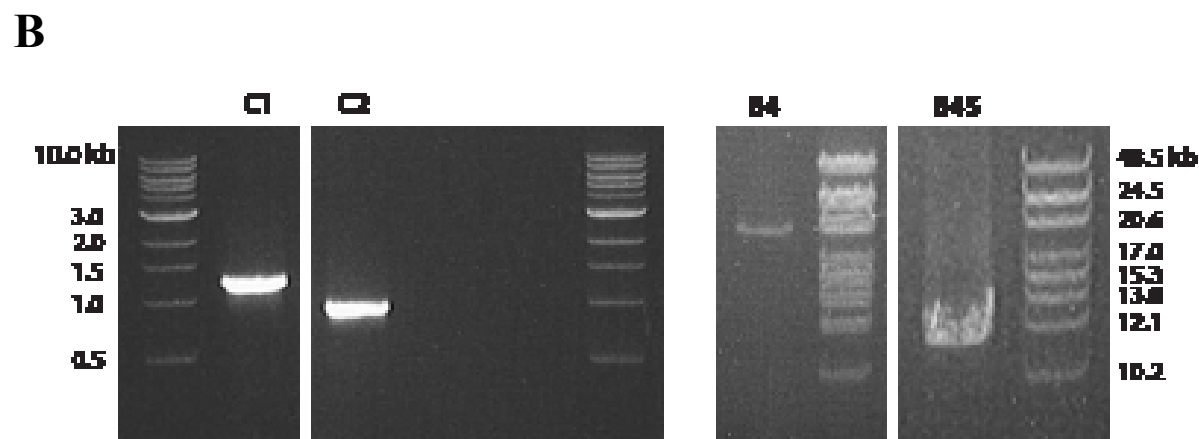
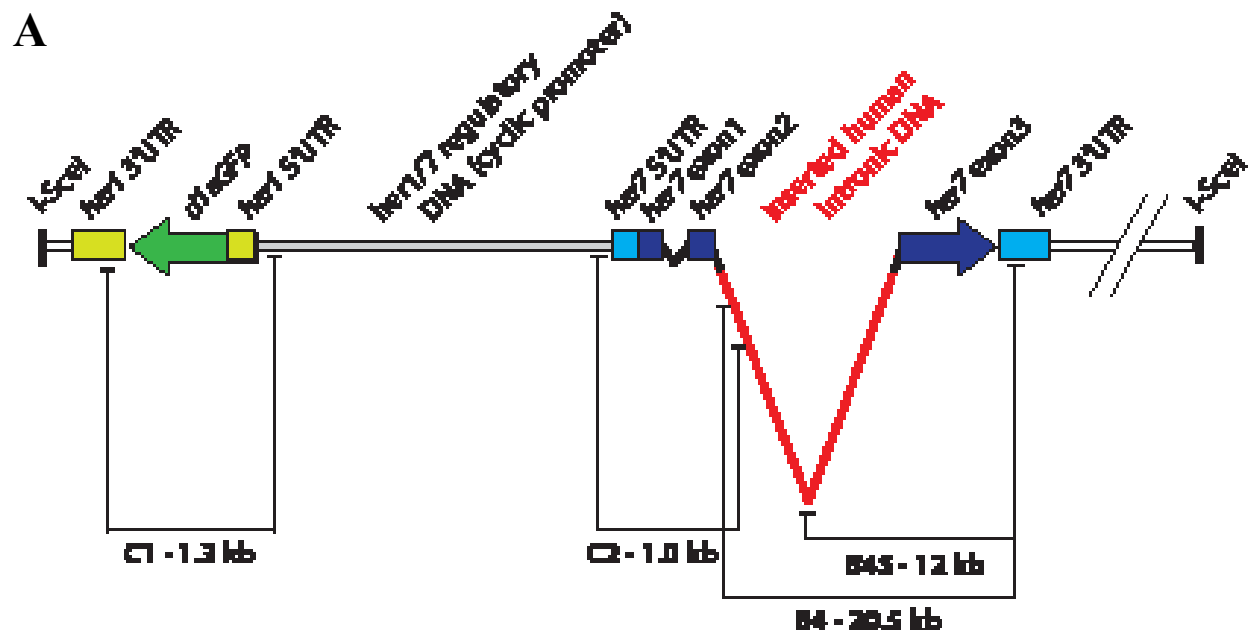


Fig. S2. PCR analysis of the integrated *her7^{b21}* transgene. (A) The *b21* BAC construct (not to scale), showing sites of PCR primers used for analysis in B. (B) PCR analysis of the DNA from a *b21* transgenic fish, demonstrating that the whole of the region including the 21 kb artificially enlarged intron is present and correctly linked to the *her1/7* cyclic promoter/enhancer. PCR primers (5'-3') were: C1forward, GCTGTCCCAACACAAATCCG; C1reverse, GAGCAGCAGAACGCCATAAG; C2forward, GCAGCTCAGGGATTGGGTTAG; C2reverse, TGCTTGGTGGCATCTGTCTG; B4forward, TGGCTTGGTCATATTGGGAAAC; B4reverse, GGATTCTGCGTGCTGCTTTC; B4Sforward, AGATGGAAGCCTGGGGAGAG; B4S reverse, GGATTCTGCGTGCTGCTTTC. These conclusions were confirmed in an independent set of PCR analyses using a different set of primers that were more closely spaced, spanning the region from the first exon of *her7* through the enlarged intron to the second exon of *her7*, in nine overlapping steps. The identities of these PCR products were checked by sequencing.

Notch signalling in an array of many cells: a model for the PSM, with noisy regulation of each *her1* and *her7* gene copy.

■ List the molecules involved and give each one an index number

```
In[2204]:= moltypes = {"g1her1", "g2her1", "g1her7", "g2her7",
  "mher1", "mher7", "pher1", "pher7", "mdelta", "pdelta", "pnicd"};
(* Prefixes g1 and g2, respectively, denote the maternal and paternal gene copies,
each of which may be in a blocked or active state
according to which regulatory proteins are bound to its
promoter. Prefix m denotes mRNA. Prefix p denotes protein. *)
nmols = Length[moltypes];
ig1her1 = 1; (* Give the molecules index numbers according
to the sequence in which they appear in the moltypes list. *)
ig2her1 = 2;
ig1her7 = 3;
ig2her7 = 4;
imher1 = 5;
imher7 = 6;
ipher1 = 7;
ipher7 = 8;
imdelta = 9;
ipdelta = 10;
ipnicd = 11;
```

■ Set the timespan of simulation and the number of elementary time-steps corresponding to one minute

```
In[2216]:= timestep = 1; (* Do not change this. (The dynamical equations assume timestep=1). To
adjust the number of minutes corresponding to a computer timestep,
change the line below, specifying the length of a minute in computer timesteps *)
minute = 4 * timestep;
tfinal = Round[1000 minute];
```

■ Define the size of the system (n1 cells x n2 cells).

```
In[2219]:= n1 = 10;
n2 = 10;
```

- **Define the geometry of the system and assign an index number to each cell. Specify the topology by listing the neighbours of each cell. Choose between cyclic and non-cyclic boundary conditions.**

```
In[2221]:= latticevector1 = N[{Sqrt[3], 0}]; (* for hexagonal lattice *)
latticevector2 = N[{Sqrt[3] / 2, 3 / 2}]; (* for hexagonal lattice *)

addresses = Flatten[Table[{ja, jb}, {ja, 0, n1 - 1}, {jb, 0, n2 - 1}], 1];
(* list of lattice addresses of the cells in the patch *)

ncells = Length[addresses];
index[{ja_, jb_}] := jb + 1 + n2 * ja;
(* serial number of cell at lattice address {ja,jb} *)

cyclicBoundaryConditions = True;
(* Set to False for non-cyclic boundary conditions, such that cells at
the edges of the n1 x n2 array have no neighbours beyond the edges *)

If[cyclicBoundaryConditions,
  neighbouraddresses[jcell_] :=
    ({j1, j2} = addresses[[jcell]]; {{Mod[j1 + 1, n1], j2},
    {Mod[j1 - 1, n1], j2}, {j1, Mod[j2 + 1, n2]}, {j1, Mod[j2 - 1, n2]},
    {Mod[j1 - 1, n1], Mod[j2 + 1, n2]}, {Mod[j1 + 1, n1], Mod[j2 - 1, n2]}}),
  neighbouraddresses[jcell_] := ({j1, j2} = addresses[[jcell]];
  Select[{{j1 + 1, j2}, {j1 - 1, j2}, {j1, j2 + 1}, {j1, j2 - 1}, {j1 - 1, j2 + 1},
  {j1 + 1, j2 - 1}}, 0 ≤ #1[[1]] ≤ n1 - 1 && 0 ≤ #1[[2]] ≤ n2 - 1 &]);

Table[neighbourindices[jcell] = Flatten[index /@ neighbouraddresses[jcell]],
  {jcell, 1, ncells}];

xyposition[jcell_] :=
  latticevector1 * addresses[[jcell, 1]] + latticevector2 * addresses[[jcell, 2]] ;
```

- **Specify default values for the lifetimes, delays, critical concentrations, and rate constants .**

Notation:

In the assignments below,

bm... denotes mRNA degradation rate (i.e. inverse of lifetime)

bp... denotes protein degradation rate (i.e. inverse of lifetime)

Values for delays and lifetimes below are loosely based on Lewis (Current Biol., 2003), Giudicelli et al. (PLoS Biol., 2007) and Ozbudak & Lewis (PLoS Genet., 2008).

```
In[2229]:= bmher1 = bmher7 = .23 / minute;
bpher1 = bpher7 = .23 / minute;
bmdelta = .23 / minute;
bpdelta = .23 / minute;
bpnicd = .23 / minute;
```

We specify the delays as a set of values $delay[[target, agent]]$, meaning that the rate of change of the “target” molecule at time t is determined by the value of the “agent” molecule at time $t - delay[[target, agent]]$. In other words, $delay[[target, agent]]$ is the delay from making a change in the quantity of *agent* to obtaining a resultant change in the quantity of *target*.

Delays may be different for actions in cis (same cell) and in trans (from neighbouring cells).

Define the tables of cis and trans delays by first setting all to zero, and then specifying values for those that are non-zero.

First index of $cisdelay[[i, j]]$ or $transdelay[[i, j]]$ specifies target, and second index specifies regulatory molecule. Since the program represents time as an integer variable, the delays must be specified as integers.


```

In[2234]:= cisdelay = Table[0, {nmols}, {nmols}] minute;

cisdelay[[imher1, ig1her1]] = cisdelay[[imher1, ig2her1]] =
  cisdelay[[imher1, ig1her7]] = cisdelay[[imher1, ig2her7]] = Round[7 minute];
cisdelay[[imher7, ig1her1]] = cisdelay[[imher7, ig2her1]] =
  cisdelay[[imher7, ig1her7]] = cisdelay[[imher7, ig2her7]] = Round[7 minute];
cisdelay[[ipher1, imher1]] = Round[1.1 minute]; (* was 2.8 min in Lewis 2003;
corrected according to RD Palmiter, Cell 1975,
data for ovalbumin synthesis in chick *)
cisdelay[[ipher7, imher7]] = Round[0.7 minute];
(* was 1.7 min in Lewis 2003; corrected according to RD Palmiter,
Cell 1975, data for ovalbumin synthesis in chick *)
cisdelay[[imdelta, ipher1]] = Round[7 minute];
cisdelay[[imdelta, ipher7]] = Round[7 minute];
cisdelay[[ipdelta, imdelta]] = Round[20 minute];

transdelay = Table[0, {nmols}, {nmols}] minute;

transdelay[[ipnicd, ipdelta]] = Round[2 minute];

maxdelay = Max[Table[{cisdelay, transdelay}, {jcell, 1, ncells}, {t, 1, tfinal}]];

```

In[2245]:=

```

hillh1 = 2; (* stoichiometry of Her1 binding to DNA *)
hillh7 = 2; (* stoichiometry of Her7 binding to DNA *)
hilln = 1; (* stoichiometry of NICD binding to DNA *)
pcrithlregg = 100; (* critical concentration of pher1 for
  binding to the her1/7 regulatory locus, in molecules per cell *)
pcrith7regg = 100; (* critical concentration of pher7 for binding
  to the her1/7 regulatory locus, in molecules per cell *)
pcritnregg = 50; (* critical concentration of pnicd for binding
  to the her1/7 regulatory locus, in molecules per cell *)
pcrithlregd = pcrithlregg; (* critical concentration of pher1 for
  inhibition of delta gene expression, in molecules per cell *)
pcrith7regd = pcrith7regg; (* critical concentration of pher7 for
  inhibition of delta gene expression, in molecules per cell *)
pcritdregn = 10000; (* a large value represents the condition that pdelta
  levels are far below the saturating level for Notch activation *)

koffgh = .5 / minute; (* koffgh is the rate constant for
  dissociation of Her protein from the her1/7 promoter/enhancer *)
(* Caution: Note that the stochastic behaviour will be misleadingly
  represented (exaggerated, in fact) if the computer timestep
  (the value of timestep above) is long compared with the equilibration time
  for the association/dissociation reaction between regulatory protein and DNA,
  i.e. long compared with 1/koffgh and/or 1/koffgn. For in that case,
  the state of the system will be updated at much less frequent intervals than
  required to follow the rapid fluctuations in the state of the gene. *)
koffgn = 1 / minute; (* koffgn is the rate constant for dissociation
  of NICD protein from the her1/7 promoter/enhancer *)
kmher1 = kmher7 = 16.5 / minute;
(* maximal synthesis rate of mher1/7 per gene copy. *)
kpher1 = kpher7 = 9.2 / minute;
(* kpher1/7 is the rate of synthesis of pher1/7 per molecule of mher1/7. *)
(* was 4.5/min in Lewis 2003; corrected according to RD Palmiter,
  Cell 1975, data for ovalbumin synthesis in chick *)
kmdelta = 33. / minute; (* maximal synthesis rate of mdelta. *)
kpdelta = 9.2 / minute;
(* kpdelta is the rate of synthesis of pdelta per molecule of mdelta. *)
(* was 4.5/min in Lewis 2003; corrected according to RD Palmiter,
  Cell 1975, data for ovalbumin synthesis in chick *)
kn = 0.1 * pcritdregn / minute; (* kn/pcritdregn is the rate of synthesis of NICD
  per molecule of pdelta when pdelta is well below its critical value *)
glher1Func = 1; (* Set to 1 for a functional gene copy,
  0 for a non-functional gene copy (i.e one that generates no transcripts). *)
g2her1Func = 1; (* Set to 1 for a functional gene copy,
  0 for a non-functional gene copy (i.e one that generates no transcripts). *)
glher7Func = 1; (* Set to 1 for a functional gene copy,
  0 for a non-functional gene copy (i.e one that generates no transcripts). *)
g2her7Func = 1; (* Set to 1 for a functional gene copy,
  0 for a non-functional gene copy (i.e one that generates no transcripts). *)
pher1Func = 1; (* Set to 1 for functional protein,
  0 for functionally null protein *)
pher7Func = 1; (* Set to 1 for functional protein, 0 for functionally null protein *)

hillh6 = 2; (* stoichiometry of Hes6 binding to DNA *)
phes6 = 100; (* Concentration of Hes6 protein in molecules per cell,
  assumed a constant in this context *)
pcrith6regg = 100;
pcrith6regd = 100;

```

■ Choose between stochastic and deterministic models.

In[2271]:= stochastic = True;

- For the **deterministic** case: use the expectation value of the state of activity of each *her1* or *her7* gene, so as to compute the smoothed-out behaviour corresponding to very rapid association/dissociation kinetics for the reaction between regulatory proteins and DNA.

We suppose we have a set of protein complexes, Pc0, Pc1, Pc2,... , which compete with one another to bind to the key regulatory site on DNA:

$G + Pc0 \rightleftharpoons GPc0$
 $G + Pc1 \rightleftharpoons GPc1$,
 etc.

Suppose furthermore that the gene is transcriptionally active in the unbound state and in the state with Pc0 bound, but otherwise is inactive. Then it is easy to show that at chemical equilibrium the expectation value of the level of gene activation is simply

$$Ng (1 + k_0 Pc_0) / (1 + k_0 Pc_0 + k_1 Pc_1 + k_2 Pc_2 + \dots)$$

where Ng is the number of gene copies and the k_i are binding constants.

■ **Specify the dynamical rules for regulation of her1 and her7 to be used in the deterministic case**

```

In[2272]:= deterministicRules =
  Hold[
    (
      f0[ig1her1, jcell_, t_, cisconcs_, rcisconcs_, rtransconcs_] :=
        (1 + (cisconcs[[ipnicd]]^hilln) / pcrithnregg) / (1 + (cisconcs[[ipnicd]]^hilln) +
          (cisconcs[[ipher1]]^hillh1) / pcrith1regg + (cisconcs[[ipher7]]^hillh7) (phes6 / pcrith6regg)^hillh6);

      f0[ig2her1, jcell_, t_, cisconcs_, rcisconcs_, rtransconcs_] :=
        f0[ig1her1, jcell_, t_, cisconcs_, rcisconcs_, rtransconcs_];

      f0[ig1her7, jcell_, t_, cisconcs_, rcisconcs_, rtransconcs_] :=
        f0[ig1her1, jcell_, t_, cisconcs_, rcisconcs_, rtransconcs_];
      f0[ig2her7, jcell_, t_, cisconcs_, rcisconcs_, rtransconcs_] :=
        f0[ig2her1, jcell_, t_, cisconcs_, rcisconcs_, rtransconcs_];
      (* Here we assume that her1 and her7 within a given copy of the her1/7
         complex are coregulated, i.e. controlled by the same regulatory DNA
         and thus always in the same state of inhibition or activation *)

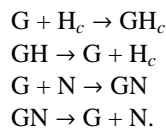
      f0[imher1, jcell_, t_, cisconcs_, rcisconcs_, rtransconcs_] := (1 - bmher1)
        cisconcs[[imher1]] + kmher1 (rcisconcs[[ig1her1]] + rcisconcs[[ig2her1]]);
      f0[imher7, jcell_, t_, cisconcs_, rcisconcs_, rtransconcs_] := (1 - bmher7)
        cisconcs[[imher7]] + kmher7 (rcisconcs[[ig1her7]] + rcisconcs[[ig2her7]]);
    )
  ];

```

■ **For the stochastic case: Calculate the transition probabilities for switching of each gene copy between active (no inhibitory protein bound) and inactive (inhibitory protein bound) states. The stochastic nature of these transitions is the source of noise in the model.**

Consider one gene copy at a time. Suppose this can exist in any one of three mutually exclusive states: with no regulatory protein bound, with NICD protein bound, or with Her protein bound, where the latter state corresponds to repression (no transcription) and the two former states correspond to active transcription. For simplicity, we assume in the first instance that Her1 protein and Her7 protein bind as multimeric complexes to DNA and that these complexes are functionally equivalent, so that the state of the gene depends simply on the sum of their concentrations, which we refer to as the amount of Her complexes in a generic sense. We also allow that NICD may function as a multimeric complex, not necessarily as a monomer.

Let G denote the gene without protein bound, N denote NICD protein complex, H_c denote Her complex, GN the gene with NICD complex bound, and GH_c the gene with Her complex bound. The various association and dissociation reactions are then:



Let p_g , p_{gn} , and p_{gh} denote the probability that the gene is in the free, NICD-bound, or Her-bound state, respec-

tively, and let N and H_c denote the concentrations of the NICD and Her protein complexes in the cell. We assume these concentrations are much greater than 1 molecule per cell, so that the association/dissociation reaction with the gene involves no significant change in the concentration of the free protein. Using a prime to denote rate of change with time, we then have the following equations:

$$p_{gh}' = p_g H_c k_{ongh} - p_{gh} k_{offgh} \quad (1)$$

$$p_{gn}' = p_g N k_{ongn} - p_{gn} k_{offgn} \quad (2)$$

$$p_g = 1 - p_{gh} - p_{gn} \quad (3)$$

The DNA-binding NICD and Her protein complexes are or may be multimeric. We assume that we are in a low-concentration regime where the concentration of n -mers is proportional to the n th power of the concentration of monomers. Thus if NICD functions as an n_N -mer, we assume N , the concentration of the active complex, is proportional to $[\text{NICD}]^{n_N}$. Likewise, we assume that H_c is proportional to $\alpha [\text{Her1}]^{n_{h1}} + \beta [\text{Her7}]^{n_{h7}}$ where α and β are constants. If, for example, Her1 binds as a homotetramer and Her7 as a dimer of heterodimers with Hes6, this latter term becomes $\alpha [\text{Her1}]^4 + \beta' [\text{Her7}]^2 [\text{Hes6}]^2$.

In the steady state,

$$p_{gh} = p_g H_c k_{ongh} / k_{offgh}$$

$$p_{gn} = p_g N k_{ongn} / k_{offgn}.$$

If we define p_{critN} as the concentration of N at which $p_g = p_{gn}$ at steady state, and p_{critH} as the concentration of H_c at which $p_g = p_{gh}$ at steady state, we have

$$k_{ongn} = k_{offgn} / p_{critN}$$

and likewise

$$k_{ongh} = k_{offgh} / p_{critH}.$$

Substituting from (3) in (1) and (2), we have

$$p_{gh}' = ((1 - p_{gh} - p_{gn}) H_c / p_{critH} - p_{gh}) k_{offgh} \quad (1')$$

$$p_{gn}' = ((1 - p_{gh} - p_{gn}) N / p_{critN} - p_{gn}) k_{offgn} \quad (2')$$

i.e., putting for short

$$H_c / p_{critH} = a,$$

$$k_{offgh} = b,$$

$$N / p_{critN} = c,$$

$$k_{offgn} = d,$$

we have

$$p_{gh}' = b * ((1 - p_{gh} - p_{gn}) a - p_{gh})$$

$$p_{gn}' = d * ((1 - p_{gh} - p_{gn}) c - p_{gn}).$$

We solve these equations for each of the three possible initial conditions $\{p_{gn}[0] = p_{gh}[0] = 0, p_{gn}[0] = 1 \text{ \& } p_{gh}[0] = 0, p_{gn}[0] = 0 \text{ \& } p_{gh}[0] = 1\}$ to obtain the probability, during one timestep of duration t , of each possible type of transition from one state of the gene to another.

```
soln0 = First[FullSimplify[DSolve[{pgh'[t] == b * ((1 - pgh[t] - pgn[t]) a - pgh[t]),
  pgn'[t] == d * ((1 - pgh[t] - pgn[t]) c - pgn[t]), pgh[0] == 0, pgn[0] == 0},
  {pgh[t], pgn[t]}, t]] (* To save unnecessarily repeating this time-
  consuming calculation every time the program is executed,
  I have performed the calculation once and,
  in a subsequent cell in the cell group,
  have defined soln0 to be equal to the resulting value. The
  initial (visible) cell of the group is now set as non-
  evaluable. Likewise for soln1 and soln2, below. *)
```

$$\left\{ \text{pgh}[t] \rightarrow \left(a e^{-\frac{1}{2} \left(b+a b+d+c d+\sqrt{-4 b (1+a+c) d+(b+a b+d+c d)^2} \right) t} \left(-\sqrt{-4 b (1+a+c) d+(b+a b+d+c d)^2} - \sqrt{-4 b (1+a+c) d+(b+a b+d+c d)^2} e^{\sqrt{-4 b (1+a+c) d+(b+a b+d+c d)^2} t} + 2 \sqrt{-4 b (1+a+c) d+(b+a b+d+c d)^2} e^{\frac{1}{2} \left(b+a b+d+c d+\sqrt{-4 b (1+a+c) d+(b+a b+d+c d)^2} \right) t} + (b (1+a+2 c) - (1+c) d) \left(-1 + e^{\sqrt{-4 b (1+a+c) d+(b+a b+d+c d)^2} t} \right) \right) \right) / \left(2 (1+a+c) \sqrt{-4 b (1+a+c) d+(b+a b+d+c d)^2} \right), \text{pgn}[t] \rightarrow \left(c e^{-\frac{1}{2} \left(b+a b+d+c d+\sqrt{-4 b (1+a+c) d+(b+a b+d+c d)^2} \right) t} \left(-\sqrt{-4 b (1+a+c) d+(b+a b+d+c d)^2} - \sqrt{-4 b (1+a+c) d+(b+a b+d+c d)^2} e^{\sqrt{-4 b (1+a+c) d+(b+a b+d+c d)^2} t} + 2 \sqrt{-4 b (1+a+c) d+(b+a b+d+c d)^2} e^{\frac{1}{2} \left(b+a b+d+c d+\sqrt{-4 b (1+a+c) d+(b+a b+d+c d)^2} \right) t} + (- (1+a) b + (1+2 a+c) d) \left(-1 + e^{\sqrt{-4 b (1+a+c) d+(b+a b+d+c d)^2} t} \right) \right) \right) / \left(2 (1+a+c) \sqrt{-4 b (1+a+c) d+(b+a b+d+c d)^2} \right) \right\}$$

■ Set soln0 to the form computed above

In[2273]:= soln0 =

$$\left\{ \text{pgh}[t] \rightarrow \left(a e^{-\frac{1}{2} \left(b+a b+d+c d+\sqrt{-4 b (1+a+c) d+(b+a b+d+c d)^2} \right) t} \left(-\sqrt{-4 b (1+a+c) d+(b+a b+d+c d)^2} - \sqrt{-4 b (1+a+c) d+(b+a b+d+c d)^2} e^{\sqrt{-4 b (1+a+c) d+(b+a b+d+c d)^2} t} + 2 \sqrt{-4 b (1+a+c) d+(b+a b+d+c d)^2} e^{\frac{1}{2} \left(b+a b+d+c d+\sqrt{-4 b (1+a+c) d+(b+a b+d+c d)^2} \right) t} + (b (1+a+2 c) - (1+c) d) \left(-1 + e^{\sqrt{-4 b (1+a+c) d+(b+a b+d+c d)^2} t} \right) \right) \right) / \left(2 (1+a+c) \sqrt{-4 b (1+a+c) d+(b+a b+d+c d)^2} \right), \text{pgn}[t] \rightarrow \left(c e^{-\frac{1}{2} \left(b+a b+d+c d+\sqrt{-4 b (1+a+c) d+(b+a b+d+c d)^2} \right) t} \left(-\sqrt{-4 b (1+a+c) d+(b+a b+d+c d)^2} - \sqrt{-4 b (1+a+c) d+(b+a b+d+c d)^2} e^{\sqrt{-4 b (1+a+c) d+(b+a b+d+c d)^2} t} + 2 \sqrt{-4 b (1+a+c) d+(b+a b+d+c d)^2} e^{\frac{1}{2} \left(b+a b+d+c d+\sqrt{-4 b (1+a+c) d+(b+a b+d+c d)^2} \right) t} + (- (1+a) b + (1+2 a+c) d) \left(-1 + e^{\sqrt{-4 b (1+a+c) d+(b+a b+d+c d)^2} t} \right) \right) \right) / \left(2 (1+a+c) \sqrt{-4 b (1+a+c) d+(b+a b+d+c d)^2} \right) \right\};$$

soln1 =

First[FullSimplify[DSolve[{pgh'[t] == b * ((1 - pgh[t] - pgn[t]) a - pgh[t]), pgn'[t] == d * ((1 - pgh[t] - pgn[t]) c - pgn[t]), pgh[0] == 1, pgn[0] == 0}, {pgh[t], pgn[t]}, t]]]

$$\begin{aligned}
\{ \text{pgh}[t] \rightarrow & \left(e^{-\frac{1}{2} \left(b+a b+d+c d+\sqrt{-4 b (1+a+c) d+(b+a b+d+c d)^2} \right) t} \right. \\
& \left(b (-1+a (-1+c) -c) \left(-1 + e^{\sqrt{(1+a)^2 b^2+2 b (-1-a+(-1+a) c) d+(1+c)^2 d^2} t} \right) + \right. \\
& (1+c)^2 d \left(-1 + e^{\sqrt{(1+a)^2 b^2+2 b (-1-a+(-1+a) c) d+(1+c)^2 d^2} t} \right) + \\
& \sqrt{(1+a)^2 b^2+2 b (-1-a+(-1+a) c) d+(1+c)^2 d^2} \\
& \left. \left(2 a e^{\frac{1}{2} \left(b+a b+d+c d+\sqrt{(1+a)^2 b^2+2 b (-1-a+(-1+a) c) d+(1+c)^2 d^2} \right) t} + \right. \right. \\
& \left. \left. (1+c) \left(1 + e^{\sqrt{(1+a)^2 b^2+2 b (-1-a+(-1+a) c) d+(1+c)^2 d^2} t} \right) \right) \right) \right) / \\
& \left(2 (1+a+c) \sqrt{-4 b (1+a+c) d+(b+a b+d+c d)^2} \right), \text{pgn}[\\
t] \rightarrow & \left(c e^{-\frac{1}{2} \left(b+a b+d+c d+\sqrt{-4 b (1+a+c) d+(b+a b+d+c d)^2} \right) t} \left(-\sqrt{-4 b (1+a+c) d+(b+a b+d+c d)^2} - \right. \right. \\
& \sqrt{-4 b (1+a+c) d+(b+a b+d+c d)^2} e^{\sqrt{-4 b (1+a+c) d+(b+a b+d+c d)^2} t} + \\
& 2 \sqrt{-4 b (1+a+c) d+(b+a b+d+c d)^2} e^{\frac{1}{2} \left(b+a b+d+c d+\sqrt{-4 b (1+a+c) d+(b+a b+d+c d)^2} \right) t} - \\
& \left. (b+a b+d+c d) \left(-1 + e^{\sqrt{-4 b (1+a+c) d+(b+a b+d+c d)^2} t} \right) \right) \right) / \\
& \left(2 (1+a+c) \sqrt{-4 b (1+a+c) d+(b+a b+d+c d)^2} \right) \}
\end{aligned}$$

■ Set soln1 to the form computed above

```

In[2274]:= soln1 = {pgh[t] -> 
$$\left( e^{-\frac{1}{2} \left( b + a b + d + c d + \sqrt{-4 b (1 + a + c) d + (b + a b + d + c d)^2} \right) t} \right. \\ \left. \left( b (-1 + a (-1 + c) - c) \left( -1 + e^{\sqrt{(1 + a)^2 b^2 + 2 b (-1 - a + (-1 + a) c) d + (1 + c)^2 d^2} t} \right) + \right. \right. \\ \left. (1 + c)^2 d \left( -1 + e^{\sqrt{(1 + a)^2 b^2 + 2 b (-1 - a + (-1 + a) c) d + (1 + c)^2 d^2} t} \right) + \right. \\ \left. \sqrt{\left( (1 + a)^2 b^2 + 2 b (-1 - a + (-1 + a) c) d + (1 + c)^2 d^2 \right)} \right. \\ \left. \left( 2 a e^{\frac{1}{2} \left( b + a b + d + c d + \sqrt{(1 + a)^2 b^2 + 2 b (-1 - a + (-1 + a) c) d + (1 + c)^2 d^2} \right) t} + \right. \right. \\ \left. \left. (1 + c) \left( 1 + e^{\sqrt{(1 + a)^2 b^2 + 2 b (-1 - a + (-1 + a) c) d + (1 + c)^2 d^2} t} \right) \right) \right) \right) / \\ \left( 2 (1 + a + c) \sqrt{-4 b (1 + a + c) d + (b + a b + d + c d)^2} \right), pgn[t] -> \\ \left( c e^{-\frac{1}{2} \left( b + a b + d + c d + \sqrt{-4 b (1 + a + c) d + (b + a b + d + c d)^2} \right) t} \left( -\sqrt{-4 b (1 + a + c) d + (b + a b + d + c d)^2} - \right. \right. \\ \left. \sqrt{-4 b (1 + a + c) d + (b + a b + d + c d)^2} e^{\sqrt{-4 b (1 + a + c) d + (b + a b + d + c d)^2} t} + \right. \\ \left. 2 \sqrt{-4 b (1 + a + c) d + (b + a b + d + c d)^2} e^{\frac{1}{2} \left( b + a b + d + c d + \sqrt{-4 b (1 + a + c) d + (b + a b + d + c d)^2} \right) t} - \right. \\ \left. \left. (b + a b + d + c d) \left( -1 + e^{\sqrt{-4 b (1 + a + c) d + (b + a b + d + c d)^2} t} \right) \right) \right) \right) / \\ \left( 2 (1 + a + c) \sqrt{-4 b (1 + a + c) d + (b + a b + d + c d)^2} \right) \};$$

```

soln2 =

```

First[FullSimplify[DSolve[{pgh'[t] == b * ((1 - pgh[t] - pgn[t]) a - pgh[t]), pgn'[t] == d *
((1 - pgh[t] - pgn[t]) c - pgn[t]), pgh[0] == 0, pgn[0] == 1}, {pgh[t], pgn[t]}, t]]]

```


$$\begin{aligned}
\{pgh[t] \rightarrow & \left(a e^{-\frac{1}{2} \left(b+a b+d+c d+\sqrt{-4 b(1+a+c) d+(b+a b+d+c d)^2} \right) t} \left(-\sqrt{-4 b(1+a+c) d+(b+a b+d+c d)^2} - \right. \right. \\
& \sqrt{-4 b(1+a+c) d+(b+a b+d+c d)^2} e^{\sqrt{-4 b(1+a+c) d+(b+a b+d+c d)^2} t} + \\
& 2 \sqrt{-4 b(1+a+c) d+(b+a b+d+c d)^2} e^{\frac{1}{2} \left(b+a b+d+c d+\sqrt{-4 b(1+a+c) d+(b+a b+d+c d)^2} \right) t} - \\
& \left. \left. (b+a b+d+c d) \left(-1+e^{\sqrt{-4 b(1+a+c) d+(b+a b+d+c d)^2} t} \right) \right) \right) \Bigg/ \\
& \left(2(1+a+c) \sqrt{-4 b(1+a+c) d+(b+a b+d+c d)^2} \right), pgn[t] \rightarrow \\
& \left(e^{-\frac{1}{2} \left(b+a b+d+c d+\sqrt{-4 b(1+a+c) d+(b+a b+d+c d)^2} \right) t} \left((1+a)^2 b \left(-1+e^{\sqrt{(1+a)^2 b^2+2 b(-1-a+(-1+a) c) d+(1+c)^2 d^2} t} \right) + \right. \right. \\
& (-1-a+(-1+a) c) d \left(-1+e^{\sqrt{(1+a)^2 b^2+2 b(-1-a+(-1+a) c) d+(1+c)^2 d^2} t} \right) + \\
& \sqrt{(1+a)^2 b^2+2 b(-1-a+(-1+a) c) d+(1+c)^2 d^2} \\
& \left. \left(2 c e^{\frac{1}{2} \left(b+a b+d+c d+\sqrt{(1+a)^2 b^2+2 b(-1-a+(-1+a) c) d+(1+c)^2 d^2} \right) t} + \right. \right. \\
& \left. \left. (1+a) \left(1+e^{\sqrt{(1+a)^2 b^2+2 b(-1-a+(-1+a) c) d+(1+c)^2 d^2} t} \right) \right) \right) \Bigg/ \\
& \left. \left(2(1+a+c) \sqrt{-4 b(1+a+c) d+(b+a b+d+c d)^2} \right) \right\}
\end{aligned}$$

■ Set soln2 to the form computed above

In[2275]:= soln2 =

$$\begin{aligned}
\{pgh[t] \rightarrow & \left(a e^{-\frac{1}{2} \left(b+a b+d+c d+\sqrt{-4 b(1+a+c) d+(b+a b+d+c d)^2} \right) t} \left(-\sqrt{-4 b(1+a+c) d+(b+a b+d+c d)^2} - \right. \right. \\
& \sqrt{-4 b(1+a+c) d+(b+a b+d+c d)^2} e^{\sqrt{-4 b(1+a+c) d+(b+a b+d+c d)^2} t} + \\
& 2 \sqrt{-4 b(1+a+c) d+(b+a b+d+c d)^2} e^{\frac{1}{2} \left(b+a b+d+c d+\sqrt{-4 b(1+a+c) d+(b+a b+d+c d)^2} \right) t} - \\
& \left. \left. (b+a b+d+c d) \left(-1+e^{\sqrt{-4 b(1+a+c) d+(b+a b+d+c d)^2} t} \right) \right) \right) \Bigg/ \\
& \left(2(1+a+c) \sqrt{-4 b(1+a+c) d+(b+a b+d+c d)^2} \right), \\
pgn[t] \rightarrow & \left(e^{-\frac{1}{2} \left(b+a b+d+c d+\sqrt{-4 b(1+a+c) d+(b+a b+d+c d)^2} \right) t} \right. \\
& \left((1+a)^2 b \left(-1+e^{\sqrt{(1+a)^2 b^2+2 b(-1-a+(-1+a) c) d+(1+c)^2 d^2} t} \right) + \right. \\
& (-1-a+(-1+a) c) d \left(-1+e^{\sqrt{(1+a)^2 b^2+2 b(-1-a+(-1+a) c) d+(1+c)^2 d^2} t} \right) + \\
& \sqrt{(1+a)^2 b^2+2 b(-1-a+(-1+a) c) d+(1+c)^2 d^2} \\
& \left. \left(2 c e^{\frac{1}{2} \left(b+a b+d+c d+\sqrt{(1+a)^2 b^2+2 b(-1-a+(-1+a) c) d+(1+c)^2 d^2} \right) t} + \right. \right. \\
& \left. \left. (1+a) \left(1+e^{\sqrt{(1+a)^2 b^2+2 b(-1-a+(-1+a) c) d+(1+c)^2 d^2} t} \right) \right) \right) \Bigg/ \\
& \left. \left(2(1+a+c) \sqrt{-4 b(1+a+c) d+(b+a b+d+c d)^2} \right) \right\};
\end{aligned}$$

Denoting the free state as the 0 state, the H-bound state as 1, and the N-bound state as 2, we have the following transition probabilities at each timestep (of duration t), with the notation $p_{01} = p[0 \rightarrow 1]$, etc.,

$p_{00} = 1 - p_{gh}[t] - p_{gn}[t]$ evaluated according to soln0 above
 $p_{01} = p_{gh}[t]$ evaluated according to soln0 above
 $p_{02} = p_{gn}[t]$ evaluated according to soln0 above
 $p_{10} = 1 - p_{gh}[t] - p_{gn}[t]$ evaluated according to soln1 above
 $p_{11} = p_{gh}[t]$ evaluated according to soln1 above
 $p_{12} = p_{gn}[t]$ evaluated according to soln1 above
 $p_{20} = 1 - p_{gh}[t] - p_{gn}[t]$ evaluated according to soln2 above
 $p_{21} = p_{gh}[t]$ evaluated according to soln2 above
 $p_{22} = p_{gn}[t]$ evaluated according to soln2 above

■ Specify the dynamical rules for regulation of *her1* and *her7* to be used in the stochastic case

```

In[2276]:= transitionProbs =
  Hold[
    (
      h1 = .;
      h7 = .;
      n = .;

      abcd = {a → ((h1 / pcrith1regg)hillh1 + (h7 / pcrith7regg)hillh7 (phes6 / pcrith6regg)hillh6),
        b → koffgh, c → (n / pcrithnregg)hilln, d → koffgn};

      soln0abcd = soln0 /. abcd;
      soln1abcd = soln1 /. abcd;
      soln2abcd = soln2 /. abcd;
      p00[h1_, h7_, n_] = 1 - pgh[t] - pgn[t] /. soln0abcd /. t → timestep;
      p01[h1_, h7_, n_] = pgh[t] /. soln0abcd /. t → timestep;
      p02[h1_, h7_, n_] = pgn[t] /. soln0abcd /. t → timestep;
      p10[h1_, h7_, n_] = 1 - pgh[t] - pgn[t] /. soln1abcd /. t → timestep;
      p11[h1_, h7_, n_] = pgh[t] /. soln1abcd /. t → timestep;
      p12[h1_, h7_, n_] = pgn[t] /. soln1abcd /. t → timestep;
      p20[h1_, h7_, n_] = 1 - pgh[t] - pgn[t] /. soln2abcd /. t → timestep;
      p21[h1_, h7_, n_] = pgh[t] /. soln2abcd /. t → timestep;
      p22[h1_, h7_, n_] = pgn[t] /. soln2abcd /. t → timestep;
    )
  ];

stochasticRules =
  Hold[
    (
      f0[ig1her1, jcell_, t_, cisconcs_, rcisconcs_, rtransconcs_] :=
        Which[
          cisconcs[[ig1her1]] == 0, RandomChoice[{
            p00[cisconcs[[ipher1]], cisconcs[[ipher7]], cisconcs[[ipnicd]]],
            p01[cisconcs[[ipher1]], cisconcs[[ipher7]], cisconcs[[ipnicd]]], p02[
              cisconcs[[ipher1]], cisconcs[[ipher7]], cisconcs[[ipnicd]]}] → {0, 1, 2}],
          cisconcs[[ig1her1]] == 1, RandomChoice[{
            p10[cisconcs[[ipher1]], cisconcs[[ipher7]], cisconcs[[ipnicd]]],
            p11[cisconcs[[ipher1]], cisconcs[[ipher7]], cisconcs[[ipnicd]]], p12[
              cisconcs[[ipher1]], cisconcs[[ipher7]], cisconcs[[ipnicd]]}] → {0, 1, 2}],
          cisconcs[[ig1her1]] == 2, RandomChoice[{
            p20[cisconcs[[ipher1]], cisconcs[[ipher7]], cisconcs[[ipnicd]]],
            p21[cisconcs[[ipher1]], cisconcs[[ipher7]], cisconcs[[ipnicd]]],
            p22[cisconcs[[ipher1]], cisconcs[[ipher7]], cisconcs[[ipnicd]]]} → {0, 1, 2}}
        ];

      f0[ig2her1, jcell_, t_, cisconcs_, rcisconcs_, rtransconcs_] :=
        Which[
          cisconcs[[ig2her1]] == 0, RandomChoice[{

```

```

    p00[cisconcs[[ipher1]], cisconcs[[ipher7]], cisconcs[[ipnicd]]],
    p01[cisconcs[[ipher1]], cisconcs[[ipher7]], cisconcs[[ipnicd]]], p02[
      cisconcs[[ipher1]], cisconcs[[ipher7]], cisconcs[[ipnicd]]] → {0, 1, 2}],
    cisconcs[[ig2her1]] = 1, RandomChoice[{
      p10[cisconcs[[ipher1]], cisconcs[[ipher7]], cisconcs[[ipnicd]]],
      p11[cisconcs[[ipher1]], cisconcs[[ipher7]], cisconcs[[ipnicd]]], p12[
        cisconcs[[ipher1]], cisconcs[[ipher7]], cisconcs[[ipnicd]]] → {0, 1, 2}],
    cisconcs[[ig2her1]] = 2, RandomChoice[{
      p20[cisconcs[[ipher1]], cisconcs[[ipher7]], cisconcs[[ipnicd]]],
      p21[cisconcs[[ipher1]], cisconcs[[ipher7]], cisconcs[[ipnicd]]],
      p22[cisconcs[[ipher1]], cisconcs[[ipher7]], cisconcs[[ipnicd]]] → {0, 1, 2}}
  ];

f0[ig1her7, jcell_, t_, cisconcs_, rcisconcs_, rtransconcs_] :=
  f0[ig1her1, jcell, t, cisconcs, rcisconcs, rtransconcs];
f0[ig2her7, jcell_, t_, cisconcs_, rcisconcs_, rtransconcs_] :=
  f0[ig2her1, jcell, t, cisconcs, rcisconcs, rtransconcs];
(* Here we assume that her1 and her7 within a given copy of the her1/7
   complex are coregulated, i.e. controlled by the same regulatory DNA
   and thus always in the same state of inhibition or activation *)

f0[imher1, jcell_, t_, cisconcs_, rcisconcs_, rtransconcs_] :=
  (1 - bmher1) cisconcs[[imher1]] + kmher1 (If[rcisconcs[[ig1her1]] = 1, 0, g1her1Func] +
    If[rcisconcs[[ig2her1]] = 1, 0, g2her1Func]);

f0[imher7, jcell_, t_, cisconcs_, rcisconcs_, rtransconcs_] :=
  (1 - bmher7) cisconcs[[imher7]] + kmher7 (If[rcisconcs[[ig1her7]] = 1, 0, g1her7Func] +
    If[rcisconcs[[ig2her7]] = 1, 0, g2her7Func]);
(* rcisconcs[[ig1her1]]==1 is the case where Her protein is bound to the gene,
   repressing it; the other cases, where the gene is free
   (rcisconcs[[ig1her1]]==0) or has NICD bound (rcisconcs[[ig1her1]]==2),
   are assumed to allow active transcription. In each case,
   the retarded value is used, reflecting the delay from
   initiation of transcription to completion of a transcript. *)
)
];

```

■ Specify the dynamical equations to be actually used

For each kind of molecule, `f0` specifies its concentration at the next time point as a function of the currently acting concentrations of the various types of molecules in the same cell (`cisconcs`) and in the neighbouring cells (`transconcs`). These “currently acting concentrations” are in general the values that were present at some earlier times, corresponding to delays in the control system, denoted by a prefix `r` (for retarded). However, sometimes - in particular when a molecule directly regulates its own synthesis, but with a delay - we may need to have `f0` depend on both the current value of a concentration (`cisconcs`) and on its retarded value (`rcisconcs`). When `f0` is called later in the program, it will be with the suitably delayed values of the concentrations as arguments. Note that the program allows for `f0` to be different in different cells and at different times.

The program allows for the dynamical rules to be position-dependent (variable from cell to cell) and/or time-dependent.

In[2278]:=

```

If[stochastic == True, ReleaseHold[stochasticRules], ReleaseHold[deterministicRules]];

f0[ipher1, jcell_, t_, cisconcs_, rcisconcs_, rtransconcs_] :=
  (1 - bpher1) cisconcs[[ipher1]] + kpher1 rcisconcs[[imher1]] pher1Func;
f0[ipher7, jcell_, t_, cisconcs_, rcisconcs_, rtransconcs_] :=
  (1 - bpher7) cisconcs[[ipher7]] + kpher7 rcisconcs[[imher7]] pher7Func;

f0[imdelta, jcell_, t_, cisconcs_, rcisconcs_, rtransconcs_] :=
  (1 - bmdelta) cisconcs[[imdelta]] + kmdelta /
    (1 + (rcisconcs[[ipher1]]hillh1 / pcrith1regd) + (rcisconcs[[ipher7]]hillh7 / pcrith7regd) (phes6 / pcrith6regg)hillh6);
f0[ipdelta, jcell_, t_, cisconcs_, rcisconcs_, rtransconcs_] :=
  (1 - bpdelta) cisconcs[[ipdelta]] + kpdelta * rcisconcs[[imdelta]];
f0[ipnicd, jcell_, t_, cisconcs_, rcisconcs_, rtransconcs_] :=
  (1 - bpnid) cisconcs[[ipnicd]] + (kn (rtransconcs[[ipdelta]] / pcrithdregn) /
    (1 + (rtransconcs[[ipdelta]] / pcrithdregn)));

```

Non-dimensionalization:

We could choose units for the protein and mRNA concentrations so as to make the critical concentrations equal to 1 (or any other value we please), for each of them, for any chosen one of its actions, leaving the other critical concentrations and the degradation rates b and the transcription initiation rates k and the cis- and trans-delays as the parameters to be explored. However, if we wish to describe events in terms of actual numbers of molecules per cell, this non-dimensionalization is not appropriate.

■ Set the starting conditions and the dimensions of the tables of values that describe the system.

fullhistory is an array of values that describes the history of the system fully, specifying the concentration of each molecule at each time point in each cell. Specifically,

fullhistory[[*t*, *jcell*, *imol*]] is the concentration of molecule *imol* in cell *jcell* at timepoint *t*.

fullhistory[[*t*]] is a snapshot of the state of the system at timepoint *t*.

recenthistory is just that part of *fullhistory* that we need to know in order to compute the next state of the system.

recenthistory[[1]] is a snapshot of the state of the system at a time preceding the present by an amount *maxdelay*;

recenthistory[[*maxdelay*+1]] is a snapshot of the present state of the system; that is,

recenthistory[[*maxdelay*+1, *jcell*, *imol*]] is the present concentration of the molecule *imol* in cell *jcell*.

In[2284]:=

```

recenthistory0 = Table[
  If[(jm == ig1her1 || jm == ig2her1 || jm == ig1her7 || jm == ig2her7), 0, 1 * RandomReal[]],
  {jt, 1, 1 + maxdelay}, {jcell, 1, ncells}, {jm, 1, nmols}];
fullhistory0 = Table[If[jt > maxdelay + 1, 0, recenthistory0[[jt, jcell, jm]]],
  {jt, 1, tfinal}, {jcell, 1, ncells}, {jm, 1, nmols}];

```

- Specify how to apply a full series of updates iteratively to obtain the full spatio-temporal history of the system as it develops subject to the chosen molecular controls, up to time tfinal.

```
In[2285]:= computebehaviour :=
(
  fullhistory = fullhistory0;
  recenthistory = recenthistory0;

  timetocompute = Timing[
    Do[
      (
        currentCisMols = Table[
          recenthistory[[1 + maxdelay, jcell, mj]],
          {itargetmol, 1, nmols}, {jcell, 1, ncells}, {mj, 1, nmols}
        ];
        (* currentCisMols[[itargetmol,jcell,mj]] is
           the current concentration of molecule #mj, in cell #jcell,
           repeated identically for all values of #itargetmol *)
        retardedCisMols = Table[
          recenthistory[[1 + maxdelay - cisdelay[[itargetmol, mj]], jcell, mj]],
          {itargetmol, 1, nmols}, {jcell, 1, ncells}, {mj, 1, nmols}
        ];
        (* retardedCisMols[[itargetmol,jcell,mj]]
           is the concentration of molecule #mj,
           evaluated with the appropriate retardation for its current (timepoint t) cis-
           action on target molecule #itargetmol, in cell #jcell *)
        retardedTransMols = Table[
          recenthistory[[1 + maxdelay - transdelay[[itargetmol, mj]], jcell, mj]],
          {itargetmol, 1, nmols}, {jcell, 1, ncells}, {mj, 1, nmols}
        ];
        (* retardedTransMols[[itargetmol,jcell,mj]] is the concentration
           of molecule #mj, evaluated in cell #jcell with the appropriate
           retardation for its current (timepoint t) trans-action on target
           molecule #itargetmol in the neighbours of cell #jcell . *)

        totNbrsRetardedTransMols = Table[
          Sum[retardedTransMols[[itargetmol, jnbr, mj]],
            {jnbr, neighbourindices[jcell]}],
          {itargetmol, 1, nmols}, {jcell, 1, ncells}, {mj, 1, nmols}
        ];
        (* totNbrsRetardedTransMols[[itargetmol,jcell,mj]] is the concentration of
           molecule #mj, evaluated with the appropriate retardation for its
           current (timepoint t) trans-action on target molecule #itargetmol,
           summed over all the neighbours of cell #jcell. *)

        newstate = Table[
          f0[imol, jcell, t, currentCisMols[[imol, jcell]],
            retardedCisMols[[imol, jcell]], totNbrsRetardedTransMols[[imol, jcell]],
            {jcell, 1, ncells}, {imol, 1, nmols}
          ];
        (* newstate[[jcell,imol]] is the concentration to be assigned
           to molecule #imol in cell #jcell at the next timepoint *)

        recenthistory = Append[Drop[recenthistory, 1], newstate];

        fullhistory[[t + 1]] = newstate;
      ),
      {t, maxdelay + 1, tfinal - 1}
    ];
    allcells = Transpose[fullhistory, {3, 1, 2}];
  ][[1]];
);
```


- Specify how to work out oscillation period, damping, amplitude, etc, from computed timecourse (for use in deterministic case only)

```
In[2286]:= printOscillationParams[tseries_, jmol_] :=
(
  m = tseries[[jmol, All]];
  Do[If[m[[n+1]] < m[[n]] && m[[n]] > m[[n-1]], (nmaxpenult = nmaxlast;
    nmaxlast = n; mmaxpenult = mmaxlast; mmaxlast = m[[n]]), {n, 2, tfinal-1}];
  Do[If[m[[n+1]] > m[[n]] && m[[n]] < m[[n-1]], (nminpenult = nminlast; nminlast = n;
    mminpenult = mminlast; mminlast = m[[n]]), {n, 2, tfinal-1}];
  period = (nmaxlast - nmaxpenult);
  ampm = mmaxlast - mminlast;
  ampdecfacm = (mmaxlast - mminlast) / (mmaxpenult - mminpenult);
  Print["For molecule ", moltypes[[jmol]],
    "\n period (in minutes) = ", N[period/minute], " last peak = ", mmaxlast,
    " last trough = ", mminlast, " peak/trough = ", mmaxlast/mminlast,
    " damping factor = ", (mmaxlast - mminlast) / (mmaxpenult - mminpenult)];
);
```

- Specify how to display the results as graphs of time course for each cell and for the mean over all cells

```
In[2287]:= printVals[listParameterNames_] := Print[Table[listParameterNames[[jlistpn]] <>
  " = " <> ToString[ToExpression[listParameterNames[[jlistpn]]]] <> " ",
  {jlistpn, 1, Length[listParameterNames]}] // TableForm];
printCisDelayTable :=
(cisDelayTable =
  Table[Flatten[{N[cisdelay[[im]] / minute], " to control " <> moltypes[[im]]}],
  {im, 1, nmols}];
Print["\nDelay (in minutes) for controlling molecule in cis\n",
  Style[TableForm[Insert[cisDelayTable, Append[moltypes, " "], 1],
  TableSpacing → {1, 1}], FontSize → 12, FontFamily → "Arial Narrow"]];
printTransDelayTable := (transDelayTable = Table[Flatten[{N[transdelay[[im]] / minute],
  " to control " <> moltypes[[im]]}], {im, 1, nmols}];
Print["\nDelay (in minutes) for controlling molecule in trans\n",
  Style[TableForm[Insert[transDelayTable, Append[moltypes, " "], 1],
  TableSpacing → {1, 1}], FontSize → 12, FontFamily → "Arial Narrow"]];
displaytimecourse :=
(
  scaling = Table[1, {nmols}];
  (* Default - subsequent lines may modify *)
  scaling[[imher1]] = 1 / 40;
  scaling[[ipher1]] = 1 / 1000;
  scaling[[ipnicd]] = 1 / 2000;
  scaling[[ipdelta]] = 1 / 1000;
  scaling[[ig1her1]] = -1;
  scaling[[ig2her1]] = -1;
  scaledAllCells = Table[scaling[[jmol]] * fullhistory[[t, jcell, jmol]],
    {jcell, 1, ncells}, {jmol, 1, nmols}, {t, 1, tfinal}];
  graph[jcell_] := ListLinePlot[scaledAllCells[[jcell, {ig1her1, imher1, ipher1,
    ipdelta, ipnicd}, All]], PlotStyle → {{RGBColor[1, 0, 0], Thickness[0.002]},
    {RGBColor[0, 1, 0], Thickness[0.002]}, {RGBColor[0, 0, 0], Thickness[0.002]},
    {RGBColor[0, 0, 1], Thickness[0.002]}, {RGBColor[1, 0, 1], Thickness[0.002]}},
  PlotRange → {{0, tfinal}, {-2, 5}}, AspectRatio → 0.6, ImageSize → 400,
  PlotLabel → (" \n g1her1 (red), mher1 (green), pher1 (black), pdelta (blue),
    pnidc (purple) \n time in minutes\n cell # " <>
    ToString[jcell] <> " at " <> ToString[addresses[[jcell]]]),
  Ticks → {Table[{100 * nt100, 100 * nt100 / minute}, {nt100, 0, tfinal / 100, 5}],
    Automatic}}];
  gt = Table[graph[njcell], {njcell, 1, ncells}];
  Print["To see time course for each cell individually,
    \n click on graph window and scroll sideways.
    \n Concentrations are scaled for convenient display. \n For g1her1,
    value 0 means the gene has no regulatory protein bound, \n
    -1 means it has Her protein bound, -2 means it has NICD bound.
    \n States 0 and -2 are transcriptionally active, state -1 is repressed."];
  Print[GraphicsRow[gt]];
  scaledMeanOverCells =
    Table[scaling[[jmol]] * (1 / ncells) Sum[fullhistory[[t, jcell, jmol]],
      {jcell, 1, ncells}], {jmol, 1, nmols}, {t, 1, tfinal}];
```

```

Print
[graphMeanOverCells =
  ListLinePlot[
    scaledMeanOverCells[{{ig1her1, imher1, ipher1, ipdelta, ipnicd}, All]],
    PlotStyle -> {{RGBColor[1, 0, 0], Thickness[0.002]}, {RGBColor[0, 1, 0],
      Thickness[0.002]}, {RGBColor[0, 0, 0], Thickness[0.002]},
      {RGBColor[0, 0, 1], Thickness[0.002]}, {RGBColor[1, 0, 1], Thickness[0.002]}},
    PlotRange -> {{0, tfinal}, {-2, 5}}, AspectRatio -> 0.6,
    ImageSize -> 400, PlotLabel ->
      ("Mean over all cells\n g1her1 (red), mher1 (green), pher1 (black),
        pdelta (blue), pnid (purple) \ntime in minutes "),
    Ticks -> {Table[{100 * nt100, 100 * nt100 / minute}, {nt100, 0, tfinal / 100, 5}],
      Automatic}]]];
graphFourierMeanOverCells[jmol_] :=
(
  m = scaledMeanOverCells[[jmol, All]];
  aft = Abs[Fourier[m]];
  maxfreq = .1 / minute;
  ListLinePlot[Take[aft, Round[maxfreq * Length[aft]]],
    PlotRange -> All, DataRange -> {0, minute * maxfreq}, AspectRatio -> 0.6,
    ImageSize -> 400, PlotLabel -> "Mean over all cells\n" <> moltypes[[jmol]] <>
      " Fourier transform; amplitude vs frequency in cycles per minute"
  )
);

```

■ Specify how to display the honeycomb pattern of cells and its coloring

```

In[2291]:= nucleardiam = .4;
membranethickness = 0.02;
intercellspace = 0.01;
redCytoplasm = imher1;
greenCytoplasm = imher1;
blueCytoplasm = ipdelta;
redNucleus = imher1;
greenNucleus = imher1;
blueNucleus = ipdelta;
colorscaling = Table[1, {nmols}];
(* Default scaling for colour display. Actual desired scaling set in next lines*);
colorscaling[[imher1]] = 20;
colorscaling[[imdelta]] = 10;
colorscaling[[ig1her1]] = .1;
colorscaling[[ipdelta]] = pcritdregn / 10;
colorscaling[[ipnicd]] = pcritnregg;
bkgrndcolor = {1, 1, 1} * 1;
cellColoring[t_] := (celljts = Table[allcells[[jcell, imol, t]] /
  (allcells[[jcell, imol, t]] + colorscaling[[imol]]), {imol, 1, nmols});
  u = addresses[[jcell, 1]];
  v = addresses[[jcell, 2]];
  membranecolor = {1, 1, 1};
  cytoplasmcolor =
    {0, celljts[[greenCytoplasm]], celljts[[blueCytoplasm]]};
  nucleuscolor =
    {0, celljts[[greenNucleus]], celljts[[blueNucleus]]}
);

centre[ni_, nj_] := ni * latticevector1 + nj * latticevector2;
hexverts = N[{{-Sqrt[3] / 2, 1 / 2}, {0, 1},
  {Sqrt[3] / 2, 1 / 2}, {Sqrt[3] / 2, -1 / 2}, {0, -1}, {-Sqrt[3] / 2, -1 / 2}}];
translate[vertexlist_, vector_] := Map[Plus[#, vector] &, vertexlist];
membrane[ni_, nj_] :=
  Polygon[translate[(1 - intercellspace) * hexverts, centre[ni, nj]]];
cytoplasm[ni_, nj_] := Polygon[
  translate[(1 - membranethickness - intercellspace) * hexverts, centre[ni, nj]]];
nucleus[ni_, nj_] := Disk[centre[ni, nj], {nucleardiam, nucleardiam}];
cell[ni_, nj_, membranecolor_, cytoplasmcolor_, nucleuscolor_] := Graphics[{
  RGBColor[membranecolor], membrane[ni, nj],
  RGBColor[cytoplasmcolor], cytoplasm[ni, nj],
  RGBColor[nucleuscolor], nucleus[ni, nj]
}];

```

```

displaySimple[t_] :=
  Show[
    Table[
      (cellColoring[t];
       cell[u, v, membranecolor, cytoplasmcolor, nucleuscolor]
      ),
      {jcell, 1, ncells}
    ],
    Background → Apply[RGBColor, bkgrndcolor],
    (*PlotRange → {{leftmargin, rightmargin}, {bottommargin, topmargin}}, *)
    AspectRatio → Automatic, PlotLabel → timelabel,
    ImageSize → 50 * {n1, n2}
  ];

displayCyclic[t_] :=
  (horizrepetition = 1;
   vertrepetition = 1;
   jhoriz = Ceiling[horizrepetition + n2 / 2];
   jvert = vertrepetition;
   leftmargin = Norm[latticevector1] * (1 + n1 * n2 / 2);
   rightmargin = Norm[latticevector1] * ((1 + jhoriz) * n1 - 1);
   bottommargin = Norm[latticevector1] * N[Sqrt[3] / 2];
   topmargin = Norm[latticevector1] * N[Sqrt[3] / 2] * ((1 + jvert) * n2 - 1);
   Show[
     Table[
       (cellColoring[t];
        Table[
          cell[u + n1 * jn1, v + n2 * jn2, membranecolor, cytoplasmcolor, nucleuscolor],
          {jn1, 0, jhoriz}, {jn2, 0, jvert}
        ]
       ),
       {jcell, 1, ncells}
     ],
     Background → Apply[RGBColor, bkgrndcolor], PlotRange →
       {{leftmargin, rightmargin}, {bottommargin, topmargin}}, AspectRatio → Automatic,
     PlotRangeClipping → True,
     PlotLabel → timelabel,
     ImageSize → 50 * {n1 * horizrepetition, n2 * vertrepetition}
   ]
  )

```

- Specify how to generate frames of a movie of the multicellular array

```

In[2317]:= makemovie[tstartshow_, tinterval_, tendshow_] :=
  Do[
    (
      timelabel = Style["t = " <> ToString[ Round[(tf - 1) / minute]] <> " minutes",
        "Section", FontSize → 14]; (* Here timelabel is defined as time elapsed since
        first time point in whole history, which therefore has timelabel 0 *)
      Print[displaySimple[tf]];
      Print[displayCyclic[tf]];
    ), {tf, tstartshow, tendshow, tinterval}
  ];

makemovieRectangle[tstartshow_, tinterval_, tendshow_] :=
  Do[
    (
      timelabel = Style["t = " <> ToString[ Round[(tf - 1) / minute]] <> " minutes",
        "Section", FontSize → 14];
      Print[displayCyclic[tf]];
    ), {tf, tstartshow, tendshow, tinterval}
  ];

makemovieSimple[tstartshow_, tinterval_, tendshow_] :=
  Do[
    (
      timelabel = Style["t = " <> ToString[ Round[(tf - 1) / minute]] <> " minutes",
        "Section", FontSize → 14];
      Print[displaySimple[tf]];
    ), {tf, tstartshow, tendshow, tinterval}
  ];

```

■ Specify any sets of variant parameters to be explored

Lists of variant values specified here for rate constants, critical concentrations and other parameters appearing in the dynamical equations are to be used in the computation, overriding default values specified earlier.

```

In[2320]:= variedParams =
  {"cisdelay[[ipdelta, imdelta]]/minute", "cisdelay[[imher1, iglher1]]/minute",
   "cisdelay[[imher7, iglher7]]/minute", "pcrithlregg", "pcrith7regg",
   "pher1Func", "pher7Func", "seedRandom", "koffgh*minute"};
variants["cisdelay[[ipdelta, imdelta]]"] = Round[{18} minute];
variants["cisdelay[[imher1, iglher1]]"] = Round[{8} minute];
variants["cisdelay[[imher7, iglher7]]"] = Round[{7} minute];
variants["pcrithlregg"] = {400};
variants["pcrith7regg"] = {400};
variants["pher7Func"] = {1, 0};
variants["pher1Func"] = {1};
variants["seedRandom"] = {4};
variants["koffgh"] = {0.5} / minute;

```

■ Do the computation and display time-course graphs and movie

Values specified here for rate constants, critical concentrations and other parameters appearing in the dynamical equations override default values specified earlier. The Do loop runs over the chosen set of different parameter choices.

```

In[2330]:= Do[
  (
    cisdelay[[ipdelta, imdelta]] = variants["cisdelay[[ipdelta, imdelta]]"][[v1]];
    cisdelay[[imher1, iglher1]] =
      cisdelay[[imher1, ig2her1]] = cisdelay[[imher1, iglher7]] =
        cisdelay[[imher1, ig2her7]] = variants["cisdelay[[imher1, iglher1]]"][[v2]];
    cisdelay[[imher7, iglher1]] = cisdelay[[imher7, ig2her1]] =
      cisdelay[[imher7, iglher7]] =
        cisdelay[[imher7, ig2her7]] = variants["cisdelay[[imher7, iglher7]]"][[v3]];
    pcrithlregg = pcrithlregd = variants["pcrithlregg"][[v4]];
    pcrith7regg = pcrith7regd = variants["pcrith7regg"][[v9]];
    pher7Func = variants["pher7Func"][[v5]];
    pher1Func = variants["pher1Func"][[v8]];
    seedRandom = variants["seedRandom"][[v6]];
    koffgh = variants["koffgh"][[v7]];

    SeedRandom[seedRandom]; (*Setting SeedRandom[n], where n is any integer,

```

```

SeedRandom[seedRandom]; (*Setting SeedRandom[n], where n is any integer,
means that the set of random numbers used in the computation subsequent
to the SeedRandom statement is reproducible,i.e the same each time the
program is run. To run the program with a different set of random numbers,
change the value of n. To make every run use a different set of random numbers,
leave the argument of SeedRandom blank,i.e write simply SeedRandom[*])
If[stochastic == True, ReleaseHold[transitionProbs], Null];
(* This statement has to be here,
and not in the earlier specification of dynamical rules, because otherwise
transitionProbs would be computed using default and not variant parameters *)

Print["\n\n-----\nFOR GRAPHS THAT FOLLOW:"];
printVals[{"moltypes", "minute/timestep", "tfinal/minute", "ncells", "hillh1",
"hillh7", "hilln", "pcrithlregg", "pcrith7regg", "pcritnregg", "pcrithlregd",
"pcrith7regd", "pcritdregn", "bmher1*minute", "bpher1*minute", "bmher7*minute",
"bpher7*minute", "bmdelta*minute", "bpdelta*minute", "bpnicd*minute",
"kmher1*minute", "kpher1*minute", "kmdelta*minute", "kpdelta*minute", "kn*minute",
"koffgh*minute", "koffgn*minute", "g1her1Func", "g2her1Func", "pher1Func",
"pher7Func", "cyclicBoundaryConditions", "seedRandom", "stochastic"}];
printCisDelayTable;
printTransDelayTable;
Print["\n\n"];
Print[ProgressIndicator[Dynamic[t], {0, tfinal}]];
computebehaviour;
printVals[{"timetocompute"}];
displaytimecourse;
printVals[variedParams];
Print["For molecule ",
moltypes[[imher7]], " (mean over all cells) \nMean over time = ",
Mean[scaledMeanOverCells[[imher7]]], " StandardDeviation = ",
StandardDeviation[scaledMeanOverCells[[imher7]]]];
If[stochastic == True, Null, printOscillationParams[scaledMeanOverCells, imher7]];
Print[graphFourierMeanOverCells[imher7]];

tstartshow = 1; (* for the movie *)
tendshow = tfinal; (* for the movie *)
tinterval = 5 minute;
Print["Colour components of cytoplasm are: \nRed = 0 x "<>
moltypes[[redCytoplasm]] <> "; Green = "<>moltypes[[greenCytoplasm]] <>
"; Blue = "<>moltypes[[blueCytoplasm]]];
Print["Colour components of nucleus are: \nRed = 0 x "<>
moltypes[[redNucleus]] <> "; Green = "<>moltypes[[greenNucleus]] <>
"; Blue = "<>moltypes[[blueNucleus]]];
makemovieRectangle[tstartshow, tinterval, tendshow]

),
{v1, 1, Length[variants["cisdelay[[ipdelta,imdelta]]"]]},
{v2, 1, Length[variants["cisdelay[[imher,igher]]"]]},
{v3, 1, Length[variants["cisdelay[[imher,igher]]"]]},
{v7, 1, Length[variants["koffgh"]]},
{v4, 1, Length[variants["pcrithlregg"]]},
{v9, 1, Length[variants["pcrith7regg"]]},
{v8, 1, Length[variants["pher1Func"]]},
{v5, 1, Length[variants["pher7Func"]]},
{v6, 1, Length[variants["seedRandom"]]}

];

```

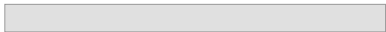
FOR GRAPHS THAT FOLLOW:

Delay (in minutes) for controlling molecule in cis

g1her1	g2her1	g1her7	g2her7	mher1	mher7	pher1	pher7	mdelta	pdelta	pnidc		
0.	0.	0.	0.	0.	0.	0.	0.	0.	0.	0.	to control	g1her1
0.	0.	0.	0.	0.	0.	0.	0.	0.	0.	0.	to control	g2her1
0.	0.	0.	0.	0.	0.	0.	0.	0.	0.	0.	to control	g1her7
0.	0.	0.	0.	0.	0.	0.	0.	0.	0.	0.	to control	g2her7
8.	8.	8.	8.	0.	0.	0.	0.	0.	0.	0.	to control	mher1
7.	7.	7.	7.	0.	0.	0.	0.	0.	0.	0.	to control	mher7
0.	0.	0.	0.	1.	0.	0.	0.	0.	0.	0.	to control	pher1
0.	0.	0.	0.	0.	0.75	0.	0.	0.	0.	0.	to control	pher7
0.	0.	0.	0.	0.	0.	7.	7.	0.	0.	0.	to control	mdelta
0.	0.	0.	0.	0.	0.	0.	0.	18.	0.	0.	to control	pdelta
0.	0.	0.	0.	0.	0.	0.	0.	0.	0.	0.	to control	pnidc

Delay (in minutes) for controlling molecule in trans

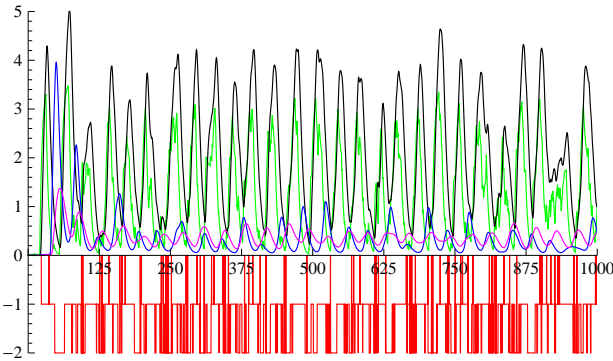
g1her1	g2her1	g1her7	g2her7	mher1	mher7	pher1	pher7	mdelta	pdelta	pnid		
0.	0.	0.	0.	0.	0.	0.	0.	0.	0.	0.	to control	g1her1
0.	0.	0.	0.	0.	0.	0.	0.	0.	0.	0.	to control	g2her1
0.	0.	0.	0.	0.	0.	0.	0.	0.	0.	0.	to control	g1her7
0.	0.	0.	0.	0.	0.	0.	0.	0.	0.	0.	to control	g2her7
0.	0.	0.	0.	0.	0.	0.	0.	0.	0.	0.	to control	mher1
0.	0.	0.	0.	0.	0.	0.	0.	0.	0.	0.	to control	mher7
0.	0.	0.	0.	0.	0.	0.	0.	0.	0.	0.	to control	pher1
0.	0.	0.	0.	0.	0.	0.	0.	0.	0.	0.	to control	pher7
0.	0.	0.	0.	0.	0.	0.	0.	0.	0.	0.	to control	mdelta
0.	0.	0.	0.	0.	0.	0.	0.	0.	0.	0.	to control	pdelta
0.	0.	0.	0.	0.	0.	0.	0.	0.	2.	0.	to control	pnid



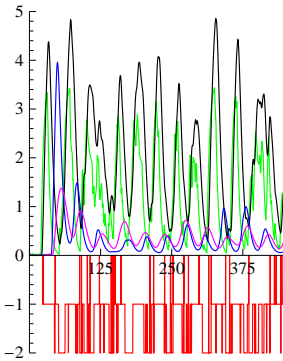
timetocompute = 1050.31

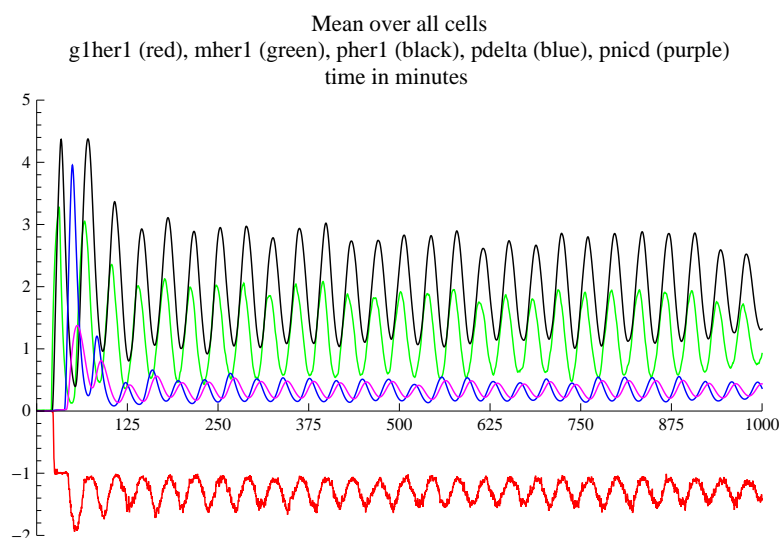
To see time course for each cell individually,
click on graph window and scroll sideways.
Concentrations are scaled for convenient display.
For g1her1, value 0 means the gene has no regulatory protein bound,
-1 means it has Her protein bound, -2 means it has NICD bound.
States 0 and -2 are transcriptionally active, state -1 is repressed.

g1her1 (red), mher1 (green), pher1 (black), pdelta (blue), pnid (purple)
time in minutes
cell # 1 at {0, 0}



g1her1 (red), mher1 (green), phe
time
cell



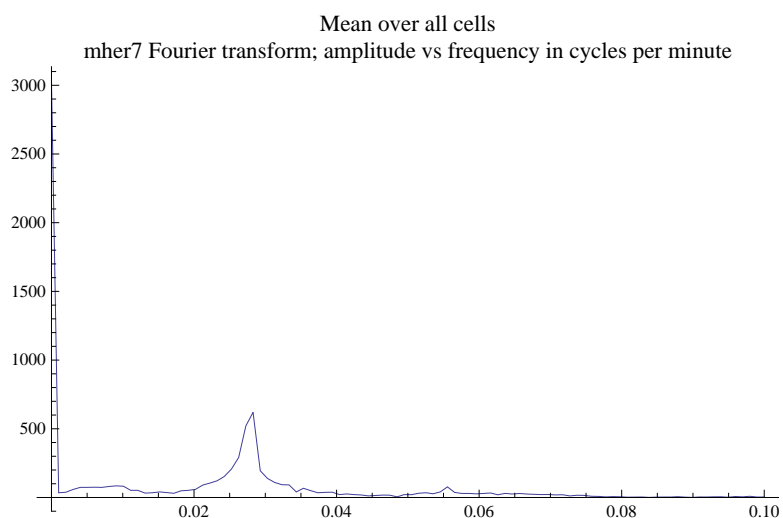


```

cisdelay[[ipdelta,imdeltal]]/minute = 18
cisdelay[[imher1,iglher1]]/minute = 8
cisdelay[[imher7,iglher7]]/minute = 7
pcrithlregg = 400
pcrith7regg = 400
pher1Func = 1
pher7Func = 1
seedRandom = 4
koffgh*minute = 0.5

For molecule mher7 (mean over all cells)
Mean over time = 47.9828   StandardDeviation = 22.7804

```



Frames of movie are deleted here to keep file size manageable, but are saved as QuickTime movie provided separately.

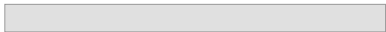
FOR GRAPHS THAT FOLLOW:

Delay (in minutes) for controlling molecule in cis

g1her1	g2her1	g1her7	g2her7	mher1	mher7	pher1	pher7	mdelta	pdelta	pnidc		
0.	0.	0.	0.	0.	0.	0.	0.	0.	0.	0.	to control	g1her1
0.	0.	0.	0.	0.	0.	0.	0.	0.	0.	0.	to control	g2her1
0.	0.	0.	0.	0.	0.	0.	0.	0.	0.	0.	to control	g1her7
0.	0.	0.	0.	0.	0.	0.	0.	0.	0.	0.	to control	g2her7
8.	8.	8.	8.	0.	0.	0.	0.	0.	0.	0.	to control	mher1
7.	7.	7.	7.	0.	0.	0.	0.	0.	0.	0.	to control	mher7
0.	0.	0.	0.	1.	0.	0.	0.	0.	0.	0.	to control	pher1
0.	0.	0.	0.	0.	0.75	0.	0.	0.	0.	0.	to control	pher7
0.	0.	0.	0.	0.	0.	7.	7.	0.	0.	0.	to control	mdelta
0.	0.	0.	0.	0.	0.	0.	0.	18.	0.	0.	to control	pdelta
0.	0.	0.	0.	0.	0.	0.	0.	0.	0.	0.	to control	pnidc

Delay (in minutes) for controlling molecule in trans

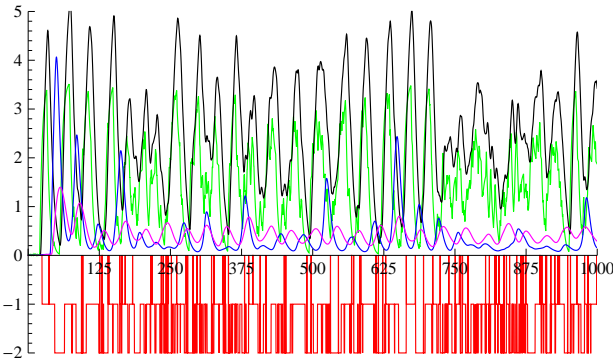
g1her1	g2her1	g1her7	g2her7	mher1	mher7	pher1	pher7	mdelta	pdelta	pnid		
0.	0.	0.	0.	0.	0.	0.	0.	0.	0.	0.	to control	g1her1
0.	0.	0.	0.	0.	0.	0.	0.	0.	0.	0.	to control	g2her1
0.	0.	0.	0.	0.	0.	0.	0.	0.	0.	0.	to control	g1her7
0.	0.	0.	0.	0.	0.	0.	0.	0.	0.	0.	to control	g2her7
0.	0.	0.	0.	0.	0.	0.	0.	0.	0.	0.	to control	mher1
0.	0.	0.	0.	0.	0.	0.	0.	0.	0.	0.	to control	mher7
0.	0.	0.	0.	0.	0.	0.	0.	0.	0.	0.	to control	pher1
0.	0.	0.	0.	0.	0.	0.	0.	0.	0.	0.	to control	pher7
0.	0.	0.	0.	0.	0.	0.	0.	0.	0.	0.	to control	mdelta
0.	0.	0.	0.	0.	0.	0.	0.	0.	0.	0.	to control	pdelta
0.	0.	0.	0.	0.	0.	0.	0.	0.	2.	0.	to control	pnid



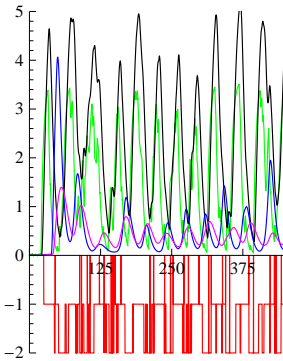
timetocompute = 1059.34

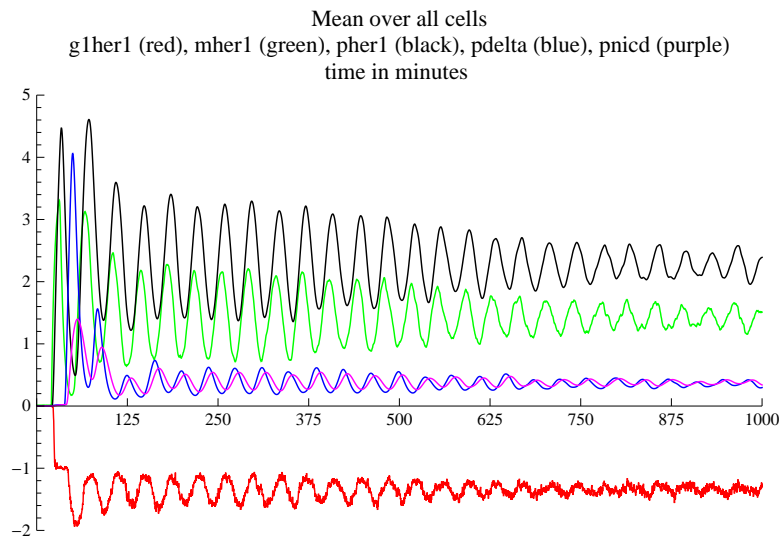
To see time course for each cell individually,
click on graph window and scroll sideways.
Concentrations are scaled for convenient display.
For g1her1, value 0 means the gene has no regulatory protein bound,
-1 means it has Her protein bound, -2 means it has NICD bound.
States 0 and -2 are transcriptionally active, state -1 is repressed.

g1her1 (red), mher1 (green), pher1 (black), pdelta (blue), pnid (purple)
time in minutes
cell #1 at {0, 0}



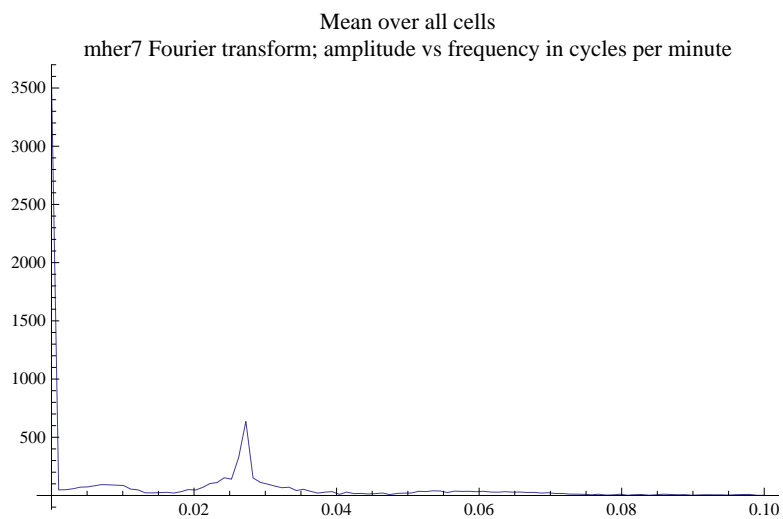
g1her1 (red), mher1 (green), phe
time
cell





```
cisdelay[[ipdelta,imdelt]]/minute = 18
cisdelay[[imher1,ig1her1]]/minute = 8
cisdelay[[imher7,ig1her7]]/minute = 7
pcrith1regg = 400
pcrith7regg = 400
pher1Func = 1
pher7Func = 0
seedRandom = 4
koffgh*minute = 0.5

For molecule mher7 (mean over all cells)
Mean over time = 56.6304   StandardDeviation = 19.429
```



In[2331]:=

Frames of movie are deleted here to keep file size manageable, but are saved as QuickTime movie provided separately.